

Journal Pre-proofs

Literature review of fatigue assessment methods in residual stressed state

Joona Vaara, Aleksi Kunnari, Tero Frondelius

PII: S1350-6307(19)31148-3

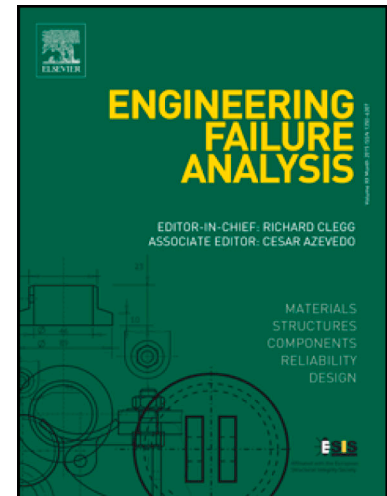
DOI: <https://doi.org/10.1016/j.engfailanal.2020.104379>

Reference: EFA 104379

To appear in: *Engineering Failure Analysis*

Received Date: 6 August 2019

Accepted Date: 6 January 2020



Please cite this article as: Vaara, J., Kunnari, A., Frondelius, T., Literature review of fatigue assessment methods in residual stressed state, *Engineering Failure Analysis* (2020), doi: <https://doi.org/10.1016/j.engfailanal.2020.104379>

This is a PDF file of an article that has undergone enhancements after acceptance, such as the addition of a cover page and metadata, and formatting for readability, but it is not yet the definitive version of record. This version will undergo additional copyediting, typesetting and review before it is published in its final form, but we are providing this version to give early visibility of the article. Please note that, during the production process, errors may be discovered which could affect the content, and all legal disclaimers that apply to the journal pertain.

© 2020 Published by Elsevier Ltd.

Literature review of fatigue assessment methods in residual stressed state

Joona Vaara^{a,*}, Aleksi Kunnari^b, Tero Frondelius^{a,c}

^aWärtsilä, Järvikatu 2-4, 65100 Vaasa, Finland

^bFinnish Defence Forces Logistics Command, P.O. Box 69, 33541 Tampere, Finland

^cMaterials and Mechanical Engineering, Pentti Kaiteran katu 1, 90014 University of Oulu, Finland

Abstract

Residual stresses remain in manufactured mechanical components after the forces related to the manufacturing process have been removed. Beneficial compressive residual stresses can be induced using shot peening, cold expansion of holes, and low plasticity burnishing, for example. The purpose of this review is to determine the relevant phenomena and fatigue assessment methodology of the residual stress state. It is shown that the common strategy for fatigue assessment – considering residual stresses simply as mean stresses – may lead to non-conservative predictions. Generalization of the presented methodologies is paid attention to and prospective research areas are indicated.

Keywords: Fatigue assessment, residual stress, partial crack closure

1. Introduction

Residual stresses can be found in the highly loaded notches due to service loading or thermomechanically induced plastification in hot components. Manufacturing always induces residual stresses in the material and stress relieving is an extra monetary cost. It is common knowledge that the poor fatigue performance of weldments is due to the tensile residual stresses. On the other hand, in highly stressed components additional safety or longer service life is desired. Purposely induced compressive residual stresses at the

*Corresponding author

Email address: joona.vaara@wartsila.com (Joona Vaara)

9 surface can be an option for improving the fatigue performance. The engi-
10 neers assessing viability of these options and fatigue performance of residual
11 stressed components are facing a non-trivial task.

12 This review aims to find out state of the art methods for assessing fatigue
13 and crack growth in residual stress fields. These reflect both finite and infinite
14 life design philosophies. Special attention is paid to generalization of the
15 presented methodology to industrial and general use. The key factors and
16 mechanisms affecting the fatigue performance, in residual stressed state, are
17 also revisited. For the sake of simplicity, welded joints were largely excluded
18 from the scope of this review, although most of the presented concepts and
19 mechanisms apply for the weldments as well. For residual stress testing
20 methods we guide the readers to the review by Withers and Bhadeshia [1].
21 Examples of failures related to residual stresses are given in the review by
22 James [2]. To better help the reader follow and form an overview, discussions
23 and summarizing is done at the end of each topic and a concluding discussion
24 is held in the end.

25 **2. Ways of producing residual stresses**

26 Residual stresses originate from spatial gradient of irreversible deforma-
27 tion and is typically result of plastification or phase transformation. Residual
28 stress is internally in equilibrium over the whole body. The peak magnitude
29 of the residual stress is typically of the order of the undeformed material's
30 yield strength [3]. In the subsection below, a few of the processes that pro-
31 duce residual stresses are briefly revisited.

32 *2.1. Peening*

33 Shot peening (SP) is the most commonly used, and most extensively stud-
34 ied, post-processing method to introduce compressive residual stresses and
35 improve fatigue performance of components. In shot peening, hard spheri-
36 cal shots are air blasted against the surface of a component. Each impact
37 point induces local plastic deformation on the surface. A plastically-stretched
38 surface attempts to expand, but the adjacent elastic region restrains the ex-
39 pansion, creating a compressive residual stress field near the surface.

40 A desirable result of shot peening is the improvement in high-cycle fatigue
41 so that crack initiation from the surface or subsurface are as probable and
42 fatigue limit increases by approximately 10–20% compared to the base mate-
43 rial, as shown by Torres *et al.* [4] for AISI 4340. In military combat aircraft

44 aluminum structures, the most relevant improvement is the increase in total
45 fatigue life, which in the best case can be several times higher in shot peened
46 material than in an as-machined condition. Further, the fatigue limit change
47 can be seen as secondary effect, because fatigue life is always finite in critical
48 aircraft structures. On the other hand, Shiozowa and Lu [5] show that for a
49 100Cr6 bearing steel that while shot peening increased the fatigue life in the
50 region above the surface fatigue limit of the material by changing the initia-
51 tion site from surface to subsurface, the very high cycle fatigue lives initiating
52 from subsurface were unaffected. A peculiarity for shot peened materials is
53 that the low-cycle fatigue performance can be worse than the base material,
54 which is attributed to the increased surface roughness, as shown by Klotz *et*
55 *al.* [6] for Inconel 718. Another characteristic of shot peening is the degree
56 of cold working. At the surface, the degree of cold working can be very high
57 (up to 30-40%) and the gradient is very steep [7]. Consequently, the depth
58 of the compressive residual stress layer is typically in range of 0.15–0.3 mm.
59 The stability of the shot peening residual stresses will be discussed later. The
60 development of numerical analysis of shot peening focuses on addressing the
61 surface coverage which largely determines the success of the treatment [8].

62 *2.2. Cold expansion of holes and interference fit fasteners*

63 Cold working of holes is also a widely used post-processing method, at
64 least in the manufacturing of aircraft structures. The basic idea of this
65 technique is to pull a mandrel through a hole (that is larger than the hole)
66 using a hydraulic puller. Temporary split-sleeves can be used in this process
67 between the mandrel and the hole or permanently installed bushings [9]. In
68 the final stage, the hole is usually reamed to ensure good surface quality.
69 This process induces a plastic deformation that increases the hole diameter;
70 however, the surrounding elastic region restricts this expansion, creating a
71 compressive residual stress field around the hole. The magnitude of the peak
72 compressive stress is roughly equal to the compressive yield stress of the
73 material. Usually, a compressive stress region spans from one radius to one
74 diameter from the edge of the hole [10].

75 Total fatigue life of the cold-worked hole is usually over three times longer
76 than that without any post-processing [11]. This yields lighter structures
77 when applied in design and production. The method can also be used in
78 service life extensions or repairs in critical holes to increase fatigue life. The
79 cold expansion process has some limitations due to high plastic deformation.
80 The process can increase the probability of stress corrosion cracking, and if

81 the hole ligament is too short, cold expansion can also fracture the parts
82 during the process. Further, operational underloads can cause limitations to
83 fatigue life improvement due to relaxation of compressive stresses [12], which
84 is discussed later.

85 Another way of producing compressive stress around a hole is to use
86 interference-fit fasteners or bushings [9]. By installing a fastener slightly
87 larger than the hole, it is possible to create a compressive stress state around
88 the hole. The drawback of this method is slightly more difficult installation
89 and removal of fasteners. In spite of this, it is still widely used in aircraft
90 structures.

91 *2.3. Laser shock peening*

92 Laser shock peening (LSP) utilizes a pulsed laser to generate a rapidly ex-
93 panding plasma burst on the part surface. An increase in pressure generates
94 a powerful compressive shockwave that propagates through the material, cre-
95 ating compressive residual stress. The plasma burst is generated from opaque
96 overlay (tape) and transparent overlay (water), which are applied on top of
97 the component for the process. LSP equipment is currently expensive; there-
98 fore, this method is not widely used. Compared to SP, this method produces
99 higher compressive residual stresses and greater surface quality. One of the
100 drawbacks of SP is the increased surface roughness. LSP, on the other hand
101 does not face this problem. The degree of cold working is typically lower
102 than in shot peening (about 9%). [7]

103 In a more recent study [13] the surface layer's microstructure was studied
104 thoroughly. High dislocation density, dislocation entanglements, slip lines
105 and very fine sub-grains were observed near the surface. Simulations of laser
106 shock peening and the formed residual stresses were utilized in [14].

107 *2.4. Low-plasticity burnishing*

108 Low-plasticity burnishing (LBP) is a relatively new post-processing method.
109 In this process, a ball or a wheel is hydraulically pressed against the treated
110 surface to induce plastic deformation on the surface. The LPB process uses
111 a fluid between the burnishing tool and the surface to avoid wearing out
112 the tool and damaging the surface. Many series of overlapping passes are
113 made until sufficient coverage is achieved. LPB can induce higher compres-
114 sive residual stresses compared to shot peening. The process helps achieve
115 minimized plasticity (no shearing due to slipping), which means that less
116 cold work (about 4%) is generated at the surface. [7]

117 The benefits of both LPB and LSP compared to traditional shot peening
 118 are deeper compressive residual stress region with less cold working, which
 119 is illustrated in Figure 1. For high temperature components, it is important
 120 that surfaces treated by LPB or LSP have higher thermal relaxation resis-
 121 tance for lower cold work and lower risk in annealing or recrystallization [7].
 122 Additionally, better improvements in fatigue performance can be achieved
 123 with these treatment methods compared to shot peening [15, 16].

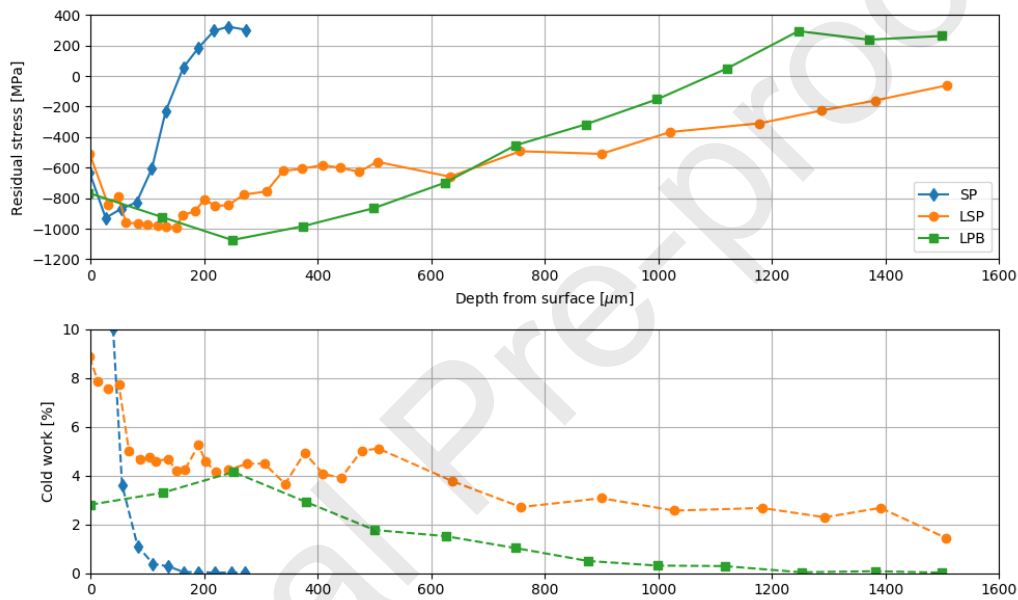


Figure 1: Residual stresses and cold work distribution in IN 718 after Shot Peening (SP), Laser Shock Peening (LSP) and Low Plasticity Burnishing (LPB). Reproduced from [7].

124 2.5. Manufacturing processes

125 There are many conventional component manufacturing processes that
 126 create residual stresses, even where that is not the primary purpose. For
 127 example, machining always produces some amount of residual stress that
 128 may be undesirable. The surface of a plain fatigue test specimen is typically
 129 electrochemically polished to eliminate unintentional effects of machining-
 130 induced residual stresses on the test results. Residual stresses can create un-
 131 desired curvature in parts, which are generally relieved using heat treatment.
 132 The machining induced residual stresses and simulation prediction methods

133 are reviewed extensively in [17] and complemented by [18, 19]. Grinding
134 related residual stresses are reviewed in [20]. Simulation of heat treatment
135 induced residual stresses are reviewed in [21] and welding in e.g. [22, 23].
136 For general overview of the role of residual stresses in fatigue of weldments
137 we guide the readers to [24]. Numerical simulation and fatigue prediction of
138 butt welding was performed in [25]. The residual stresses of dissimilar steel
139 joints were considered in [26]. For more recent fatigue assessment methods
140 the continuum damage model was applied in [27, 28], the latter considering
141 the effect of porosity as well as residual stresses.

142 There are many other manufacturing processes or surface treatments that
143 produce residual stresses and affect the fatigue life of the component, such
144 as forging, casting, induction- and case-hardening, and deep rolling. For the
145 sake of simplicity, in the manuscript these processes are not discussed in
146 depth.

147 **3. Stability of residual stresses**

148 In the previous section, the causes of residual stresses were explained, and
149 understanding them is crucial for understanding the mechanisms affecting
150 the stability of residual stresses. In principle, relaxation of residual stresses
151 always brings the neighboring material elements stress-free configurations
152 closer, meaning it relieves the internal imbalance. This section is largely
153 based on the extensive and recent review by McClung on the stability of
154 residual stresses [3]. It is evident that the stability of residual stresses is
155 crucial for the fatigue performance of components. This is highlighted in
156 Kim *et al.*'s studies on the relaxation of residual stresses of shot-peened
157 medium-carbon steel under rotating bending fatigue tests [29, 30]. Kim *et al.*
158 *al.* proposed that the fatigue crack growth in their experimental scenario
159 starts only after the residual stresses have relaxed to below 80% of their initial
160 value. McClung in his review stated, 'complete or nearly complete relaxation
161 of residual stresses is rare and occurs only for severe cycling, sometimes with
162 an additional influence from elevated temperature.' McClung categorized
163 the types of relaxations into four categories, which are elaborated in the
164 next subsection.

165 *3.1. Static loading*

166 The initial residual stress tends to relax by quite a large amount during
167 the first load cycle in operation. The amount of relaxation depends on the

168 magnitude and direction of loading with respect to the residual stresses. The
 169 dependence on direction of loading can be explained by Bauschinger's ef-
 170 fect [31, 32, 7, 33], where the yield surface of a plastically-deformed material
 171 translates towards the stress state that caused the irreversible deformation.
 172 The sign of residual stress in this deformed material is typically the opposite
 173 of the loading that caused it. As the yield surface has translated, yielding
 174 can be expected earlier if the load is in the opposite direction of the irre-
 175 versible deformation, and later if it is to the same direction. If loaded in an
 176 opposite direction to the irreversible deformation, and yielding occurs, the
 177 internal imbalance is alleviated and the residual stresses relaxed. In other
 178 words, compressive residual stresses tend to be more stable in tensile op-
 179 erating loading conditions and vice-versa [3]. Occasional overloads are also
 180 considered to belong to this category. These findings were also reported by
 181 Toribio *et al.* [34, 35] with the FEA of cold-drawn wires. Stefanescu [12]
 182 showed for cold-worked holes that underloads significantly relaxed the initial
 183 compressive residual stress field. McClung notes that modeling this should
 184 be rather easy considering the knowledge available on initial residual stress
 185 state and service loading [3].

186 3.2. Cyclic loading

187 Residual stresses tend to relax with applied mechanical loading cycles.
 188 Kodama [36] measured residual stress relaxation on the surface of shot-
 189 peened specimens and proposed a model where the cyclic relaxation of resid-
 190 ual stresses is linear with respect to the logarithmic number of cycles. The
 191 slope term depends on the applied stress amplitude. Kim *et al.* [29] docu-
 192 mented the relaxation of shot peening-induced residual stresses thoroughly,
 193 and the corresponding data as well as their empirical model (1) is visualized
 194 in Figure 2.

Kim *et al.* proposed an empirical model to characterize the experimental
 data

$$\sigma_{res}(\sigma_a, N) = (1.50\sigma_Y - 2.75\sigma_a) + (-0.75\sigma_Y + 0.91\sigma_a) \log N, \quad R = -1, \quad (1)$$

195 where σ_Y is the material's yield strength, σ_a is the applied stress amplitude,
 196 and N is the number of fatigue cycles. McClung notes in his review that no
 197 general model exists for modeling the relaxation of residual stresses [3]. Klotz
 198 *et al.* [6] and Kirk [37] reported initial compressive residual stress becoming
 199 tensile with high stress fatigue cycles. Wagner and Luetjering [38] concluded

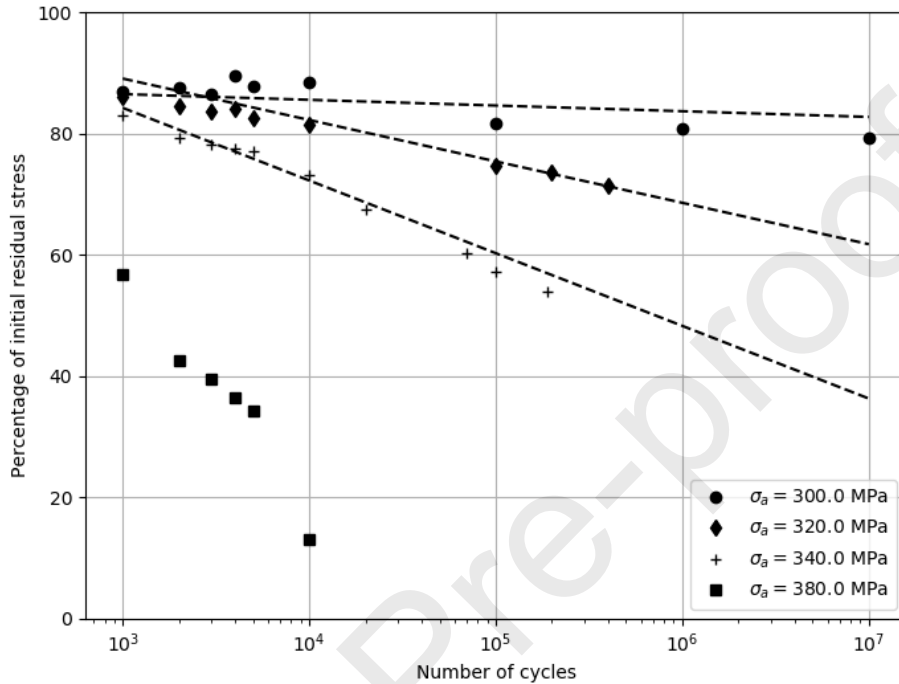


Figure 2: Percentage of initial residual stress versus number of rotating bending fatigue cycles ($R=-1$) in shot peened 0.45% carbon steel specimen. The dashed lines are the model (1) predictions. Reproduced from [29] using average curves.

200 that the cyclic stability of residual stresses depends on the material hardening
 201 or softening with the fatigue cycles.

202 3.3. Thermal effects

With an increase in temperature, materials tend to become softer, and the dislocation movement is easier. Creep-like mechanisms, and dislocation glide and climbing, gradually activate with temperature. Metallurgists have taken advantage of this in the process of stress relieving because it is designed to relax the induced residual stresses from manufacturing. Vöhringer *et al.* studied the relaxation of shot peening residual stresses at different annealing temperatures between 20°C and 600°C as a function of time up to 60,000 minutes for the titanium alloy Ti-6Al-4V. They found that a significant relaxation occurred at temperatures above 300°C [39]. They proposed

an Avrami-type equation to describe the observed phenomena

$$\frac{\sigma_{res}(T)}{\sigma_{res}(243K)} = \exp [-(At)^m], \quad (2)$$

where the value of m is determined by the corresponding relaxation mechanism, and parameter A follows an Arrhenius-type equation

$$A = B \exp \left[\frac{-Q}{kT} \right], \quad (3)$$

203 where B is a constant, Q is the activation energy, k is Boltzmann's constant,
 204 and T is the absolute temperature. They fit the model to the experiments
 205 and found the effective activation energy to be $Q = 2.78\text{eV}$. They also
 206 found this value to correspond to the activation energy of α -titanium's high
 207 temperature creep and self-diffusion with a reference value of $Q = 2.51\text{eV}$,
 208 and concluded the dominating relaxation mechanism to be climbing of edge
 209 dislocations. [39]

210 The model (2) predictions using mean parameter values and data from
 211 [39] are shown in Figure 3.

212 3.4. Crack extension effects

213 Fukuda and Yasuyuki [40] experimentally studied the redistribution of
 214 welding residual stresses due to crack growth in JIS SS41 mild steel. They
 215 showed that the tensile residual stresses redistributed remarkably with fatigue
 216 crack propagation. They also concluded that it was indeed the crack exten-
 217 sion, and not the cyclic loading, that was responsible for the redistribution.
 218 Lee *et al.* [41] also studied the phenomenon with mild steel SS330 and weld-
 219 ing tensile residual stresses. They also observed the substantial redistribution
 220 of residual stresses with fatigue crack propagation. Lam and Lian [42] stud-
 221 ied the effect of residual stress redistribution with crack extension of 2024-T3
 222 aluminum specimen. The specimen had compressive residual stresses and no
 223 significant effect of residual stress redistribution was observed. As an expla-
 224 nation, they suggested that their experimental setup had low residual stresses
 225 compared to the applied external loads and that with higher magnitude of
 226 residual stresses, the effect could be more significant. Pavier *et al.* [43]
 227 studied the role of residual stresses in cold-worked holes. Even though they
 228 performed sophisticated finite element analyses that could take into account
 229 the redistribution of residual stresses, they did not draw any conclusions on

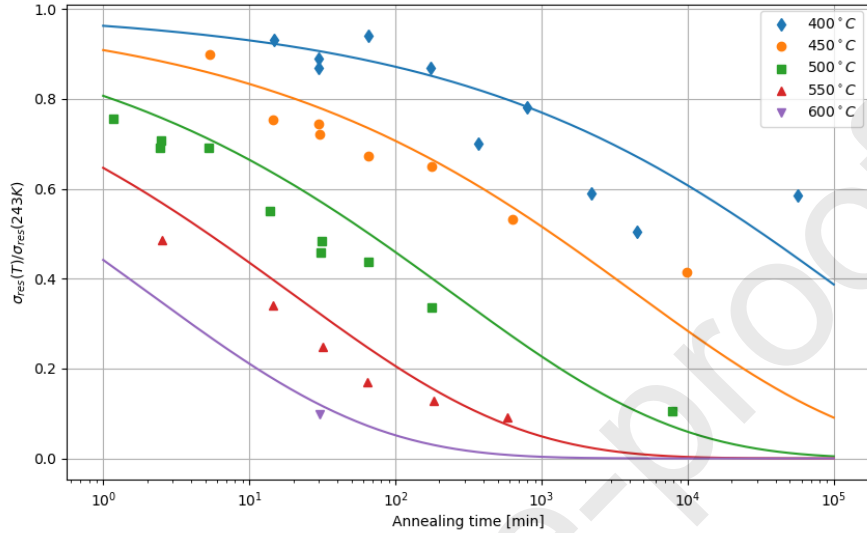


Figure 3: Percentage of initial residual stress versus annealing time at different temperatures for shot peened Ti-6Al-4V. Reproduced from [39]. Model predictions using mean parameter values.

230 the redistribution. However, they did demonstrate static stress distributions
 231 at different applied loading levels and introduced crack. We would like to
 232 note that a cyclic analysis, and perhaps even a crack growth scheme, should
 233 be applied to get simulation estimates. On top of this, the unloaded state
 234 of stresses should be visualized to show the effect of crack growth to the
 235 compressive residual stress redistribution.

236 Nelson [44] commented on the measurements by various authors in which
 237 growing the crack through an initial compressive residual stress field resulted
 238 in an increase in crack growth rate (compared to the residual stress-free
 239 measurements), but only after the crack had grown through the compressive
 240 residual stress field and most of the original tensile residual stress field. They
 241 suggested a possible explanation to this being the redistribution of the resid-
 242 ual stresses with crack growth, which occurred when the crack extended to
 243 the tensile residual stress region. This would then effectively drop the crack
 244 opening stress levels. Nelson could have been right to predict what other
 245 researchers later suggested to be partial crack opening [31, 45] that resulted
 246 in the net increase of effective stress intensity range in situations where the

247 crack grows in residual stress gradient.

248 Özdemir and Edwards [10] studied the relaxation of residual stresses of
249 cold-worked hole on 7050-T76 aluminum alloy. At fatigue limit, they ob-
250 served almost full relaxation of the surface residual stresses. Below the sur-
251 face, the maximum compressive residual stress reduced from -500 MPa to
252 -400 MPa. The residual stress profile eventually stabilized at the fatigue
253 limit. They reported inlet side cracks arrested to approximately 1 mm in
254 length and suggested that the relaxation was primarily due to crack growth.

255 Amjad *et al.* [46] recently studied experimentally the residual stress re-
256 laxation of cold-worked holes in the presence of a fatigue crack. They used
257 thermoelastic stress analysis as well as synchrotron X-ray diffraction and
258 concluded that the fatigue crack did not significantly relax or redistribute
259 the compressive residual stress field by cold working.

260 We could not find clear measurements or simulations of significant com-
261 pressive residual stress redistribution with the fatigue crack extension, given
262 near-threshold or small-scale yielding loading levels. For tensile residual
263 stresses in welding, these effects are more pronounced. A simple explana-
264 tion would be that the introduction of a crack prevents stresses from passing
265 through the interface in tension but does not in compression.

266 4. Cold-working effects on fatigue strength

267 Most of the methods producing residual stresses also, as a byproduct, pro-
268 duce cold work in the material. By cold working we mean microstructural
269 changes due to plastic deformation or increase in dislocation density, typi-
270 cally indicated as either hardening or softening. Kliman *et al.* [47] collected
271 the work of other researchers who performed fatigue tests with prestrain,
272 i.e., a specimen without residual stresses but with microstructural changes
273 due to cold working. The collection is shown in Figure 4, and it emphasizes
274 the potential importance of this phenomenon. While several materials show
275 a positive slope, there are exceptions where the fatigue limit is drastically
276 reduced even with a small amount of prestrain. Wagner and Luetjering [38]
277 performed interesting studies on Ti-6Al-4V, such as rotating bending fatigue
278 tests for five different conditions: electropolished, shot-peened, shot-peened
279 and annealed (nearly complete residual stress relief), shot-peened and elec-
280 tropolished (20 μm), and, finally, shot-peened, annealed, and electropolished
281 (20 μm) specimen. The results are compiled in Table 1. The 10^7 fatigue
282 strength for different configurations were 700, 720, 370, 845, and 800 MPa,

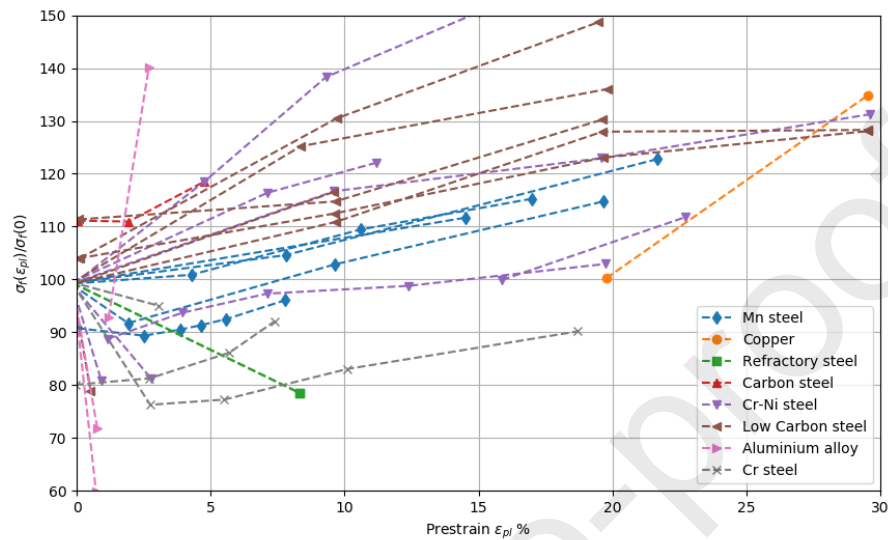


Figure 4: Relative change in fatigue limit due to cold working for various materials. Reproduced from [47] (original data from various sources).

283 respectively. The annealing reduced the 10^7 fatigue strength from 720 to 370
 284 MPa, even though all of the fatigue cracks in their studies initiated from the
 285 surface. The annealed and electropolished condition regained 430 MPa of
 286 the fatigue strength to a value of 800 MPa, which is higher than for the shot-
 287 peened condition. This find was attributed to the easy initiation of cracks
 288 from the rough surface produced by shot peening. The shot-peened and elec-
 289 tropolished surface had the highest fatigue strength. The fatigue strength
 290 of shot-peened, annealed and electropolished surface was approximately 100
 291 MPa higher than that of only electropolished, which was deduced as being
 292 because of cold working.

293

294 The phenomena presented until now have mainly concerned the fatigue
 295 crack initiation. The following two chapters deal with phenomena concerning
 296 the fatigue crack growth emphasized in residual stressed state: crack closure
 297 and non-elliptical shaped cracks.

Table 1: The fatigue strength of Ti-6Al-4V in various surface conditions [38].

Condition	Fatigue strength [MPa]
Electropolished	700
Shot-peened	720
Shot-peened and annealed	370
Shot-peened and electropolished	845
Shot-peened, annealed and electropolished	800

298 5. Crack closure

299 The crack closure is currently seen as the dominant explanatory factor for
300 the stress ratio dependencies in crack growth rates and threshold values. As
301 the residual stresses can be seen to modify the effective stress ratio, a short
302 review of the phenomenon is seen necessary here. Elber [48] noticed the
303 compliance curve in a cracked body being nonlinear with changes in loading
304 in elastic region – indicating varying load carrying geometry. In his Ph.D
305 thesis, he proposed that a plastic wake is left behind a propagating fatigue
306 crack tip that should result in a crack closure during unloading the speci-
307 men under macroscopic tensile loading. Measurements were set up to prove
308 their hypothesis and it was concluded that, indeed, the crack in the fatigue
309 specimen was fully open only for a part of the tensile load cycle. Previously,
310 it was thought that closure could only occur under macroscopic compressive
311 loading. Since then, crack closure has been under active investigation by
312 several authors. This finding gave rise to the need for defining the opening
313 stress of the crack to be able to outline the effective stress intensity range pre-
314 cisely. We shall introduce the key concepts without being too critical of the
315 relative contributions. The readers are guided towards the recent review of
316 related phenomenon by Pippin and Hohenwarter [49], and for near-threshold
317 behavior the review by Suresh and Ritchie [50]. A couple of highlights are:

- 318 • Five distinct sources of crack closure were identified: plasticity, oxide,
319 roughness, viscous fluid, and phase transformation [50]
- 320 • Crack closure is more present in plane stress conditions than in plane
321 strain conditions [51, 52, 53]
- 322 • Physically-short crack growing from a notch does not initially exhibit
323 crack closure, resulting in higher crack growth rates [49]

- 324 • Overload crack growth delayed retardation can be understood with
325 temporary removal of crack closure due to crack tip blunting [49, 54]
- 326 • Finite element analyses suggest that different standard crack growth
327 test specimen exhibit different degrees of crack closure [55]

328 The magnitude of crack closure can be experimentally determined using
329 compliance techniques, crack propagation techniques, and non-mechanical
330 contact measurements [49]. Another way of determining the amount of crack
331 closure is through Finite Element Analysis (FEA). McClung and Sehitoglu
332 [53, 56] wrote an early review of the modeling. Pommier and Bompard [57]
333 studied the effect of Bauschinger effect on the plasticity-induced crack closure
334 and concluded that there was a strong interaction between the material's
335 cyclic plastic behavior and the observed stress ratio, overload and underload
336 effects. A more recent work was conducted by Camas *et al.* [58]. The
337 essential learnings of the work were on the choice of elasto-plastic constitutive
338 model, crack advancing scheme, and mesh refinement compared to crack
339 growth rate and size of plastic zone.

340 Pommier *et al.* [59] reported sensitivity of the crack opening load to the
341 minimum load at the negative stress ratios for N18 superalloy, and the detri-
342 mental effect of high compression on the fatigue crack growth rates. The
343 results are shown in Figure 5. It can be seen that the crack opening load
344 was found to be negative for high applied compression. When the magni-
345 tude of the compression reduced at $R = -1$, the crack opening load became
346 similar to that measured at $R \approx 0$. They reached a good agreement with
347 the measured opening levels with FEA. Silva [60] reported the crack closure
348 concept as being inadequate in explaining the observed crack growth rates
349 at $R = -1$. They performed fatigue crack growth tests for various mate-
350 rials and found that as the maximum applied load increased, the opening
351 load decreased; however, for some materials the crack growth rate did not
352 change accordingly. For cyclically hardening materials, the crack growth
353 rate increased with the increase of maximum load (which was the case for
354 Pommier), whereas for cyclically softening materials, the reverse occurred.
355 For materials that exhibit neither cyclic hardening nor softening, the crack
356 growth rates were insensitive to the load amplitude. Using the sizes of mono-
357 tonic and cyclic plastic zones of Rice [61], they rationalized that for negative
358 load ratios the role of cyclic plastic material behavior was emphasized. They
359 then suggested that the materials' varying degrees of Bauschinger effect could

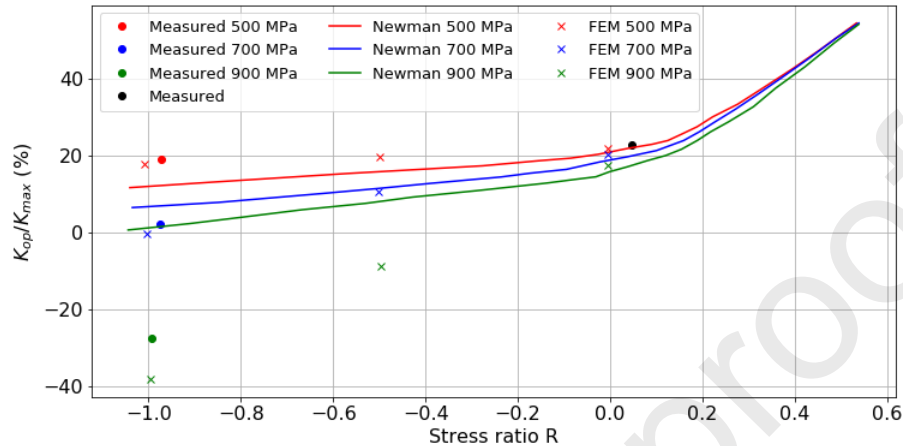


Figure 5: Evolution of the estimated crack opening stress intensity factor as function of stress ratio and maximum stress. Reproduced from [59].

360 explain the phenomenon; high Bauschinger effect would cause cyclic plasti-
 361 fication ahead of the crack tip during compression and relax the effective
 362 compressive residual stresses. Thus, the compression at $R = -1$ would be
 363 detrimental to the materials exhibiting high Bauschinger effect. We would
 364 like to note that based on the measurements of Pommier, and the explana-
 365 tion offered, it may be safe to assume that the importance of this effect is
 366 diminished at load levels near crack growth threshold. So, an analogy to the
 367 lack of cyclic residual stress relaxation at fatigue limit can be inferred here.

368 The studies performed on fatigue crack growth retardation due to over-
 369 loads are interesting in light of residual stresses. The role of plasticity-
 370 induced crack closure and residual stresses in overload related crack growth
 371 retardation is still under active discussion [54, 62]. Jones [63] studied the
 372 strain-hardening effect on un-notched fatigue crack growth of Ti-6Al-4V.
 373 Understanding that annealed material hardens with plastic deformation, his
 374 original hypothesis was that the overload retardation effect could be partly
 375 explained by strain hardening. The strain hardening, however, increased the
 376 crack growth rate and could not thus explain the overload retardation. Robin
 377 *et al.* [64] performed experimental studies on single-overload fatigue crack re-
 378 tardation and concluded that the effective stress intensity factor due to crack
 379 closure, measured by compliance method, could not produce the observed

380 transient crack growth behavior, when the crack growth rate was recover-
381 ing from the overload retardation. They also found that a better agreement
382 with the experimental data could be reached by calculating residual stresses
383 due to the overload. Shercliff and Fleck [65] reached similar conclusions re-
384 garding the assessment based on crack opening stress after overload being
385 non-conservative. Based on FEA, they suggested the reason for the discrep-
386 ancy was the partial closure of the crack. Paris *et al.* [66] proposed a simple
387 model for partial crack closure modifications to the effective stress intensity
388 range that was later modified by Borrego *et al.* [67] to provide a smoother
389 transition from the overload as a function of crack length.

390 Salvati *et al.* [54] attempted to separate the effects of crack closure and
391 residual stresses after an overload by testing first at high load ratio (0.7)
392 to induce crack growth without crack closure, which was verified by in-situ
393 Digital Image Correlation (DIC). Following the overload the strain distribu-
394 tion was quantified with synchrotron to calibrate an elastoplastic FE-model.
395 Tests with lower load ratio (0.1) were also performed and crack closure was
396 observed before the overload and to a greater extent after the overload. The
397 crack growth rate of the closure-free test ($R=0.7$) quickly returned (after
398 half of the overload plastic zone size) to the pre-overload steady-state val-
399 ues. With the lower load ratio test ($R=0.1$), where closure was present, the
400 crack growth retardation effect after the overload lasted longer. It was then
401 inferred from the experimental crack growth rates, calibrated FE-model and
402 in-situ DIC measurements, that the two effects were similar in magnitude but
403 the closure contributed over a longer distance after the overload. Thielen *et*
404 *al.* [62] studied the near crack tip stress fields of overloaded and baseline
405 crack growth specimens with in-situ synchrotron and concluded that directly
406 after the overload the residual stresses have dominant role in explaining the
407 crack growth behavior.

408 For negative applied stress ratios, Halliday *et al.* [68], Makabe *et al.* [69]
409 and Silva [70] reported an overall acceleration of crack growth after overload,
410 as opposed to the expectation of retardation, for certain materials, both
411 in plane stress and plane strain. Halliday considered short cracks whereas
412 Makabe and Silva considered long cracks. FEA performed by Halliday could
413 predict the changes in residual stresses ahead of the crack tip, which was
414 in agreement with the observed crack growth behavior. Silva found for cer-
415 tain materials almost no effect of overloads or underloads at negative base
416 load ratios, and also concluded that the materials' cyclic plastic properties—
417 Bauschinger effect in particular—seemed to control the crack growth behav-

ior at negative stress ratios. Silva emphasized that the crack closure, or any other proposed mechanism, could not explain the observed behavior, and suggested that, although crack closure could explain most features of the fatigue crack growth, it should be considered more as a consequence rather than a cause. It should be noted that as Silva and Pommier previously reported the sensitivity of the crack opening loads to the maximum compression (or load amplitude) at negative stress ratios, no consideration was made for the effect of base load amplitude on the phenomenon here. Given the explanation of cyclic plasticity, the crack growth rate should naturally, as in the case of non-overload negative stress ratio findings, approach the findings of $R = 0$ with decreasing load amplitudes.

Suresh and Ritchie [50] argued that the intrinsic crack length dependence due to crack closure breaks the similitude concept of fracture mechanics. They discouraged the interpretation of fracture mechanical data using nominal ΔK -based concepts due to loss of uniqueness, not representing the true crack driving force. Their proposed solution was to develop analyses capable of capturing the mechanics of fatigue crack: cyclic plasticity, non-stationary crack tip fields, and crack closure. *"Until such analyses are available, the use of ΔK_{eff} , representing closure-adjusted ΔK values, provides probably the most fundamental approach, at least for academic assessment of fatigue behavior"*, they concluded. Vasudevan and Sadananda have also raised concern on focusing what is happening behind the crack tip instead of the crack tip internal stresses (see e.g. [71]). Vasudevan *et al.* [72] and Suresh [50] have criticized the difficulties of determining unique crack closure levels.

6. Non-elliptical shaped cracks

Pell *et al.* [73] studied crack growth rate from a cold-worked hole made in aluminum alloy. They noticed that without cold working, the cracks were elliptical. They also noticed a difference in the mandrel entry and exit face crack lengths. The crack had grown into a shape what they called "bulbous nose". The crack depth on entry and exit side of cold-expanded (C-E) hole as a number of flights, corresponding loading spectrum repetitions, are shown in Figure 6. The control group had no cold-expansion treatment and the crack growth can be found to be several times faster. Kokaly *et al.* [74] made similar observations for cold-worked holes. They noticed that with increased thickness of the plate, the relative difference of crack growth rates between the entry and exit faces increased. They performed FEA to analyze

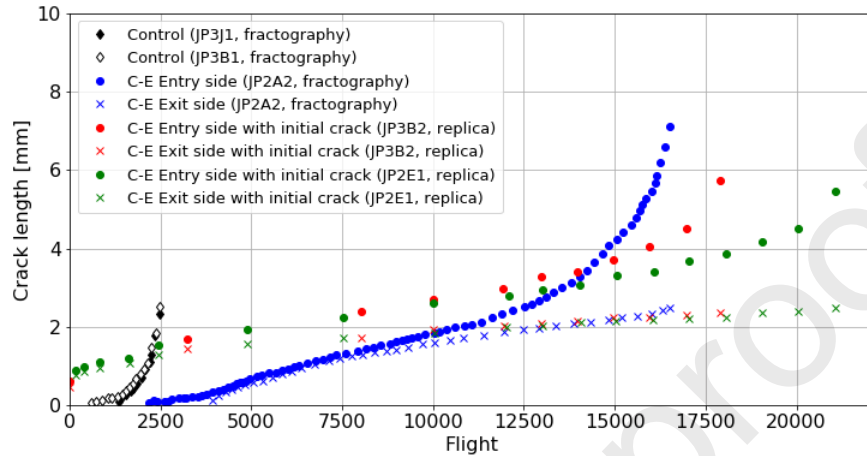


Figure 6: Crack growth on entry and exit sides of a hole subjected to aircraft loading spectrum repetitions. Reproduced from [73].

454 the residual stress state and an analysis on crack growth, and found that
 455 the non-symmetric distribution of the residual stresses in the radial direction
 456 could explain the phenomenon. McClung [3] commented on the finding by
 457 Prev y *et al.* [15] in which they made an artificial semi-circular crack using
 458 electrical discharge machining (EDM) for IN718 alloy and grew the crack in
 459 fatigue up to certain length, after which they applied low plasticity burnish-
 460 ing on the surface. The crack that grew after the treatment was found to
 461 be of a peculiar shape. Liu *et al.* [75] used a cohesive zone model-based
 462 approach to study in 3D the crack propagation in a shot-peened specimen.
 463 They also could observe non-elliptical cracks in their simulation with the
 464 presence of the residual stresses. They, however, could not produce experi-
 465 mental verification for their model. Many authors above argued for the need
 466 for improved analysis capabilities beyond just assuming the elliptical crack
 467 shapes in these situations.

468 7. Fatigue assessment

469 Thus far, we have discussed ways of producing residual stresses, the sta-
 470 bility of residual stresses, and effects of cold working for the fatigue strength.
 471 Browsing through literature, many of these phenomena were studied sepa-
 472 rately. The majority of the studies are experimental in nature, and little

473 effort went into the predictions that would assist the practical engineering
474 work. Depending on the end destination for the component with residual
475 stress treatment, either stress life (SN-curve) or fatigue crack growth rate
476 are typically measured. These two schools are also present in making the
477 fatigue assessments; crack initiation and fracture mechanical crack growth
478 approaches. The former typically aims to study changes in the fatigue limit
479 (infinite life design philosophy) whereas the latter aims to primarily study
480 changes in the fatigue crack growth rate (finite life design philosophy).

481 *7.1. Fatigue crack initiation*

482 Most of the approaches aimed for assessing fatigue crack initiation treat
483 the residual stresses as mean stresses. Much like in fatigue, no general work-
484 flow seems to overshadow the others, but instead, every researcher uses their
485 favored fatigue criteria. Let us next describe some of the fatigue assessment
486 methods proposed for residual stressed states. We shall only consider publi-
487 cations where the fatigue assessment was performed with a goal of predicting
488 or reflecting to the observed fatigue behavior. The prediction error used here
489 is the relative difference of the predicted and measured values. The models
490 are not explicitly written to avoid the vast amount of parameters to be in-
491 troduced. Instead, the workflows are described and the reader is given the
492 references to follow for further reading.

493 Leitner *et al.* [76] recently performed induction hardening simulations for
494 50CrMo4 to simulate the induced residual stress field. The fatigue assess-
495 ment was performed on basis of linear-elastic stress analysis combined with
496 the Ramberg–Osgood relationship to correct the strain amplitude from the
497 linear-elastic stress amplitude. After this, they combined the Smith, Watson
498 and Topper (SWT) damage parameter [77] with the total strain life formula
499 by Manson, Coffin and Basquin. The damage parameter considers maximum
500 principal stress and principal strain range on the maximum principal strain
501 range plane. The parameters were derived from the local hardness measure-
502 ments and uniform material law described in [78]. They performed fatigue
503 tests using notched specimen and got a decent match with the fatigue life
504 prediction. However, the model could not capture the measured fatigue limit.
505 No consideration was made for the redistribution of the residual stresses.

506 Kliman *et al.* [47, 79] described a workflow for finding the optimal param-
507 eters for the cold-worked hole. Their model is based on Haigh diagram and
508 identifying changes that can be applied to it. They considered microstruc-
509 tural changes due to cold working as shown in Figure 4, changes in surface

roughness and surface properties, residual stresses acting as mean stress, material's sensitivity to mean stress (i.e. slope of the Haigh diagram), cyclic material properties, and secondary factors such as strain ageing. They did point out the uncertainty with the assumption of the cold-working effects measured for uniaxially stressed specimen, because most of the real surface residual stress methods yield biaxial stretch (and thus biaxial residual stresses). They verified the proposed model with aluminum alloy Al-Cu-Mg, for which the cold working had a negative effect on fatigue limit. They were able to estimate optimal residual strain in good agreement with the measured values.

Fathallah *et al.* [80] studied the high-cycle fatigue prediction using Crossland and Dang Van criteria [81] for shot-peened SAE 3415 notched flat three-point bending specimen. The stress ratio used in the tests was $R = 0.1$. They modeled the shot peening defects (called superficial damage in the paper) using the principles of continuum damage mechanics by Lemaitre [82] to lower the fatigue limit at the surface. A modification to the fatigue limit was applied to account for cold working as a power-law function of the ratio of the width of the diffraction peak at half the maximum value of diffraction (FWHM), which is commonly considered to be a measure of the amount of cold work. The work-hardening coefficient was chosen as the exponent of the power-law measured from the tensile test mechanical response. They noted that the cold working correction factor was very close to unity for this material due to the work-hardening coefficient. The stress concentration due to surface imperfections of the successive shot peening indentations was simulated using FEA based on the shot radius and exposure time. The fatigue limits were calculated using the as-machined fatigue tests and the fatigue limit at stress ratio $R = -1$ was estimated using the empirical relationship given by Gerber. The superficial damage was calibrated to the measured fatigue strengths under different peening conditions and fatigue criteria. We would like to comment that without the use of this superficial damage, the prediction errors increase to 6.4%. Furthermore, choosing the Goodman diagram to predict the fatigue limit at stress ratio $R = -1$, instead of Gerber, causes the prediction error to rise to 85.9%. The choice of Gerber's mean stress correction here effectively suppresses the mean stress sensitivity. The ratio of fatigue limit at stress ratio $R = -1$ and ultimate tensile strength using the Gerber diagram is 0.29, which is low for mild steel (typically values in the range of 0.4-0.5 should be expected, see e.g. [83, Chapter 6, p. 291]) (ultimate tensile strength was reported to be 510 MPa). Had the fatigue

548 limit at stress ratio $R \leq -1$ been measured, the described assessment would
549 have been more assuring.

550 Fernandez Pariente and Guagliano [84] performed rotating bending fa-
551 tigue tests for 42CrMo4 steel with three different surface treatment condi-
552 tions: gas nitrided, gas nitrided + shot-peened, and gas nitrided + shot-
553 peened + partly stress-relieved. They introduced a small artificial crack in
554 the specimen in an attempt to control the initiation site. The residual stresses
555 were measured in each condition. They also measured the micro-hardness
556 distributions along the depth of the material. All of these were measured
557 both before and after the test using run-out specimen. Following Murakami
558 [85], they applied the common fracture mechanics-based approach and found
559 that only the gas-nitrided prediction was inside 10% error margin (predicted
560 13.9 vs measured 14.2 MPam^{1/2}). The prediction errors for the other two
561 conditions were approximately -35%. They argued that the measured micro-
562 hardness could not describe the cold-working effects of shot peening because
563 no substantial difference could be observed between the nitrided and nitrided
564 + shot-peened conditions. On the other hand, the FWHM values were differ-
565 ent for different treatments. Inspired by the work of [80] they then extended
566 Murakami's prediction formula to take into account the changes in the sur-
567 face FWHM values. This correction provided a vastly enhanced prediction
568 capability as the prediction errors were within 2% error margin.

569 Albizuri *et al.* [86] performed thorough measurements for 34CrNiMo6-
570 QT steel in machined, polished, shot-peened and low plasticity burnished
571 conditions. The fatigue performance was measured with $R = -1$ rotating
572 bending tests where relaxation of the residual stresses and surface finish-
573 ing quality were measured. The fatigue limit improved by 39% from the
574 machined for the shot-peened specimen and 52% for the LPB'd specimen,
575 whereas the polished specimen reached similar fatigue performance with the
576 shot-peened specimen. They used von Mises effective stable residual stress
577 and Dietmann's mean stress fitting criterion to reach agreement with the ob-
578 served fatigue limit improvements for the LPB treatment and did not include
579 cold working effects.

580 Bagherifard *et al.* [87] combined Taylor's theory of critical distances
581 (TCD) [88] with the Sines fatigue criterion [89] to predict the fatigue limit of
582 shot-peened notched and smooth 40NiCrMo7 specimen in rotating bending,
583 and notched specimens in axial fatigue tests. The axial fatigue tests were
584 performed using load ratio $R = 0.1$ and the mean stress sensitivity param-
585 eter was calibrated to these two load ratio results. They further modified

586 the fatigue limits based on the measured surface roughness [90] and, based
587 on the measured FWHM values, the cold working hardening correction, as
588 described in [84]. They noticed that using the measured biaxial residual
589 stress as the mean stress (hydrostatic stress) resulted in significantly higher
590 prediction error (23.7% on average for rotating bending tests) compared to
591 treating the compressive residual stresses as uniaxial in the cyclic stress am-
592 plitude direction (-5.5% on average for rotating bending tests and 3.9% for
593 the axial tests). The biaxial residual stress with Sines criterion resulted in
594 non-conservative predictions. The reason for this was not elaborated. In the
595 same paper, they used fracture mechanics-based Atzori approach, described
596 in [91]. For this approach, they approximated the fatigue limit mean-stress
597 sensitivity using Morrow approximation. The prediction errors were on an
598 average -16.8% for the axial tests, overestimating the differences between the
599 different peening conditions and resulting in overly conservative predictions.
600 The reason for this was thought to be the relaxation of residual stresses. We
601 would like to comment that the measured differences in the FWHM values,
602 and thus the cold working effect, between the peened and un-peened condi-
603 tions were practically nonexistent, unlike for [84], especially considering the
604 unreported measurement uncertainty.

605 In the second part of the study by Bagherifard *et al.* [92], a local fatigue
606 limit concept by Eichseder [93] considering the stress gradient was extended
607 with surface-roughness correction and cold-working effect. The prediction
608 errors with this procedure were on an average -16% for the rotating bending
609 tests and 9% for the axial tests. They also performed calculations according
610 to the FKM guidelines described in [94] using both the nominal and local
611 stress approaches. The nominal stress approach had an average prediction
612 error of -4.4% for the rotating bending tests and -4.5% for the axial tests.
613 The local stress approach in turn had average prediction errors of -5.6% and
614 -10.2%, respectively.

615 Gerin *et al.* [95, 96] studied fatigue behavior of forged surface with var-
616 ious surface conditions. The residual stresses due to shot blasting and shot
617 peening were measured. The surface profiles were scanned, fatigue loading
618 modeled using elastic FEM and the fatigue performance analyzed using Dang
619 Van fatigue criterion combined with TCD. The Dang Van parameters were
620 fit to give the best overall agreement with the experimental results. The
621 prediction results were roughly contained within $\pm 15\%$ error margins.

622 The approaches are compiled in Table 2. Some researchers used the very
623 surface stresses of shot peening indentations analyzed by FEA, whereas oth-

Authors	Specimen	Material	Fatigue criterion	Conditions	Relaxation	Cold-working	Surface roughness	Mean stress	Notes
[76]	Notched Four-point bending	50Cr-Mo4	SWT	Induction hardened	No	Yes	No	Uniaxial $\sigma_{max} = \sigma_a + \sigma_{res}$	Crack initiation in the hardened high-cycle fatigue
[47, 79]	Cold hole expansion	Al-Cu-Mg	Haigh diagram	Cold hole expansion	No, discussed	Literature	No	Uniaxial Haigh diagram	Workflow to optimize parameters on idea level
[80]	Notched Three-point bending R=0.1	SAE 3415	Crossland Dang Van	Machined Shot-peened	Neglected	FWHM	SEM idealized FEM	Hydrostatic Gerber	Great extrapolation in mean stress assessed
[84]	Sandglass Rotating bending Artificial micro-hole	42Cr-Mo4	Murakami	Nitrided Nitrided+Shot-peened +Partly stress relieved	Measured	FWHM	Artificial micro-hole	Murakami Effective R	Measured HV to explain the observed working effects.
[86]	Smooth Rotating bending	34CrNiMo6	Basquin	Machined Polished shot-peened low-plasticity burnished	Measured	No	Measured	Von Mises Dietmann	Model for residual stress relaxation
[87, 92]	Notched and smooth Rotating bending Axial R=0.1	40NiCrMo7	Sines+TCD Atzori Eichlseeder FKM	Machined Shot-peened	Neglected	FWHM	Measured Literature	Hydrostatic Uniaxial Measured Morrow	Hydrostatic stress resulted in non-conservative estimates
[95, 96]	Smooth flat Plane bending Axial R=-1	C70	Dang Van+TCD	Polished stress-relieved as forged forged + shot-peened forged + shot-blasted	Neglected	Neglected	Scanned FEM/Peterson	Hydrostatic	Fatigue criterion best fit to all measurements

Table 2: Compilation of fatigue assessment approaches in the literature.

624 ers were driven towards less local approaches, such as TCD or approaches
625 that include a stress gradient correction factor. Some of these criteria use
626 hydrostatic stress as a measure of mean stress with varying success, whereas
627 other criteria only considered the residual stress in the direction of the uni-
628 axial loading. The mean stress sensitivity of the material's fatigue strength
629 is naturally pronounced, and it would be preferable to measure the fatigue
630 strength at compressive mean stresses instead of extrapolating with one of the
631 classic mean stress models. Majority of the studies neglected relaxation or
632 redistribution of the residual stresses, especially when predicting fatigue limit
633 was the goal. Cold working effects were generally accounted for; however,
634 only one of the studies mentioned above used measured data for the effects
635 on fatigue limit. The other approaches to take into account the cold work-
636 ing were largely phenomenological and perhaps specific to the material. The
637 Vickers hardness in Murakami's formula could not capture the cold working
638 effects but the FWHM could. Cold working generally increases the surface
639 roughness, and models capturing these effects were widely used. We would
640 like to note that this emphasizes the complexity of the phenomenon, and
641 not a single study was found where all of the ingredients were systematically
642 measured and then combined to make a fatigue prediction model. Until then,
643 uncertainty will always be present, and no generalization of the approach can
644 be made to account for different materials and differences between the test
645 specimen and the real components.

646 *7.2. Fatigue crack growth rate*

647 The traditional engineering fatigue analysis procedure has two main phases:
648 1) crack initiation analysis using stress- or strain-life-based methods and 2)
649 crack growth analysis using fracture mechanics-based methods. After the
650 initiation of the fatigue crack, the interest naturally shifts to the questions
651 – how critical is the crack, how fast does the crack grow, and will it stop?
652 In the presence of residual stresses, some interesting phenomena in crack
653 growth, such as emphasized crack closure, partial crack opening, and non-
654 elliptical-shaped cracks, were reported.

655 In the following subsection, we discuss some of the most common strate-
656 gies for fracture mechanics-based crack-growth prediction methods.

657 *7.2.1. Superposition principle*

The superposition principle of linear elastic fracture mechanics (LEFM)
has been utilized for its simplicity. In superposition principle, complex load-

ing is divided into simpler loadings that have known stress intensity factor solutions, and the contribution of each load ingredient to the stress intensity factor, analyzed separately, is summed up. Another key concept is Bueckner's weight functions [97], which allows analyzing any kind of loading once the weight functions for the geometry are known. The analysis in residual stressed state typically uses weight functions to integrate over the crack flank for the effect of residual stresses on the stress intensity factor K_I^R at the crack tip, as shown in (4). We follow Parker [98] in the description of the analysis process

$$K_I^R = \int_a p(x)m(x, a)dx, \quad (4)$$

where $p(x)$ is the residual stress acting on the crack line of an un-cracked body and $m(x, a)$ is the weight function. Then, the effective stress intensity range ΔK and load ratio R are determined. For the case where the minimum stress intensity factor due to the external load $K_{I_{\min}}^L$ added to the residual stress intensity factor is positive ($K_{I_{\min}}^L + K_I^R > 0$), we get:

$$\Delta K = K_{I_{\max}}^L - K_{I_{\min}}^L \quad (5)$$

$$R = \frac{K_{I_{\min}}^L + K_I^R}{K_{I_{\max}}^L + K_I^R} \quad (6)$$

And for the case where the minimum stress intensity factor is negative ($K_{I_{\min}}^L + K_I^R \leq 0$)

$$\Delta K = K_{I_{\max}}^L + K_I^R \quad (7)$$

$$R = 0 \quad (8)$$

Effective R -method involves measuring the crack growth curves with different R -ratios, and either having the parameters interpolated or using some model taking into account the changes in R -ratio. Parker [98] found that, in the case of partially closed crack, a check was to ensure that the crack flank displacement field was non-overlapping

$$v(x, a) = \frac{2}{H} \int K_I(a)m(x, a)da, \quad (9)$$

658 where H is an elastic constant depending on whether the study is in plane-
 659 strain or plane-stress conditions. If nonphysical overlapping is found, then
 660 a nonlinear contact pressure acting on the crack flanks should be iterated

661 until the crack flanks do not overlap anymore. Although the contact pres-
662 sure is dependent on the displacement of the crack flanks, it does not violate
663 the principles of superposition. Todoroki and Kobayashi [99] showed this
664 methodology in action and found that its predictions were in good agreement
665 with the FEA model as well as the measurements for S35C steel. Beghini and
666 Bertini [100] came to similar conclusions with a C-Mn steel. In more recent
667 analyses, FEM has been utilized to account for the contact of the crack flanks
668 as well as possible residual stress redistribution with the crack growth [101].
669 Good agreement with measurements was reached for LSP-treated AA2024-
670 T3 CT-specimen's crack growth rates in [14] where the crack growth rates
671 were fit to the unpeened crack growth rate. Pavan *et al.* [101] performed
672 crack growth tests for AA2524-T351 aluminium alloy middle-crack tension
673 specimen with and without LSP-treatment. Similar to Keller *et al.* [14],
674 the prediction based on LEFM, superposition principle and rigid contact of
675 the crack faces in FE-analysis yielded the best agreement with the measure-
676 ments. All above mentioned successful use of superposition principle include
677 through-plate crack configuration.

678 Concerns have been raised over the validity of the superposition princi-
679 ples not accounting for residual stress redistribution as the crack propagates
680 through the residual stress field, which may result in non-conservative pre-
681 dictions [41, 42, 43]. The answer to this has been the use of FEM to naturally
682 include possible redistribution of the residual stresses [101]. Some authors
683 have suggested that superposition could not take into account partial clo-
684 sure of the crack [102], which, as pointed out by Parker [98], is not true.
685 The reader is suggested to read the lengthy discussion between Nelson and
686 Parker [103] on arguments presented in Nelson's article [44]. The proposed
687 limitation of $R \geq 0$ set by Parker clearly do not take into account the more
688 recent findings on negative applied stress ratios [59, 57, 60, 70].

689 To take into account the overload-related crack retardation effects without
690 macroscopic residual stresses, empirical models by Wheeler [104] or Willen-
691 borg [105] are commonly used. According to these models, retardation occurs
692 while the crack tip plastic zone is within the overload plastic zone. The Wil-
693 lenborg model predicts a residual stress intensity factor generated by the
694 overload, and utilizes it in the superposition principle to define an effective
695 stress ratio. Although we could not find use of these models in macroscopic
696 residual stress fields, in principle, if the overload modifications to the original
697 residual stress field can be approximated, then the workflow described above
698 should yield results that are in agreement with the principles of Willenborg

699 model.

700 Based on the findings, we note that the superposition principle combined
 701 with the weight functions is an effective tool for analyzing the stress intensity
 702 factors of residual stresses. More recent analyses utilize FEM for account-
 703 ing for the contact of crack flanks and possible redistribution of the residual
 704 stresses. Typically, in practical engineering scenarios, only mode I loading
 705 with one-dimensional residual stress field is used. However, the weight func-
 706 tions can be used for modes II and III as well. Weight functions generally do
 707 exist for 3D, but are restricted to elliptical-shaped cracks.

708 7.2.2. Models for crack closure and findings in residual stress fields

The crack closure approach attempts to capture the crack opening/closing stresses in order to get a physically-accurate effective stress intensity factor range that drives crack growth. Crack opening stress is a function of the effective stress ratio R and can be defined experimentally or numerically, as discussed earlier. The effective stress intensity range then becomes:

$$\Delta K_{I_{\text{eff}}} = K_{I_{\text{max}}} - K_{I_{\text{op}}}, \quad (10)$$

709 where $K_{I_{\text{op}}}$ is the crack opening stress intensity factor. The main idea is that
 710 there exist intrinsic parameters that form a master curve for the crack growth,
 711 and the conditions at the crack tip vary due to crack closure. Characterizing
 712 the crack closure and using $\Delta K_{I_{\text{eff}}}$ should then fall to the master curve under
 713 all conditions. The crack closure approach has been considered superior for
 714 crack growth analysis in weldments [3]. It can also be used more flexibly to
 715 analyze effects of load history [44]. Based on his measurements on 2024-T3
 716 aluminum alloy, Elber [106] proposed an empirical relationship between the
 717 ratio of the closure intensity factor and maximum intensity factor as a func-
 718 tion of load ratio. Modifications to this relationship have been proposed by
 719 various other authors. Newman [52] developed an analytical Dugdale-type
 720 model to calculate the crack opening stresses, and found that the predictions
 721 of crack growth rates were in good agreement with the experimental data.
 722 Later, on the basis of FE analyses, Newman provided an empirical model to
 723 predict the crack opening stress [107], which was popularized in NASGRO
 724 model by Forman and Mettu [108]. Pommier *et al.* [59] proposed modifica-
 725 tion to the Newman's model to cover the load level dependence at negative
 726 stress ratios. The difference in crack opening predictions was attributed to
 727 the differences in the constitutive modeling. Newman used a perfectly plastic

728 material model in his analyses, which was unable to capture the Bauschinger
 729 effect.

730 In macroscopic residual stress fields, Mukai *et al.* [109] reported that
 731 a crack growing through a compressive residual stress field to the tensile
 732 residual stress field cannot be explained with the conventional crack opening
 733 load. A compliance curve with an unusual shape, where the unloading and
 734 loading paths were different, was observed by several authors [45, 31], and
 735 they suggested partial crack closing behavior as the cause of this observation.
 736 A workflow was proposed to define the effective stress intensity range based
 737 on the partial crack closure stress intensity $K_{I_{part,op}}$, which is defined from
 738 the measured compliance curve [109]. The measurement data from Kang *et al.*
 739 *et al.* [45] is visualized in Figure 7. Kang *et al.* [45] found a good agreement
 740 between their measurements and this method. Choi and Song [31] performed
 741 FEA to simulate the effect. They replicated the asymmetric loading and
 742 unloading behavior of the crack tip opening and closing, but found that
 743 the simulated crack mouth closing value was in good agreement with the
 measured partial opening value.

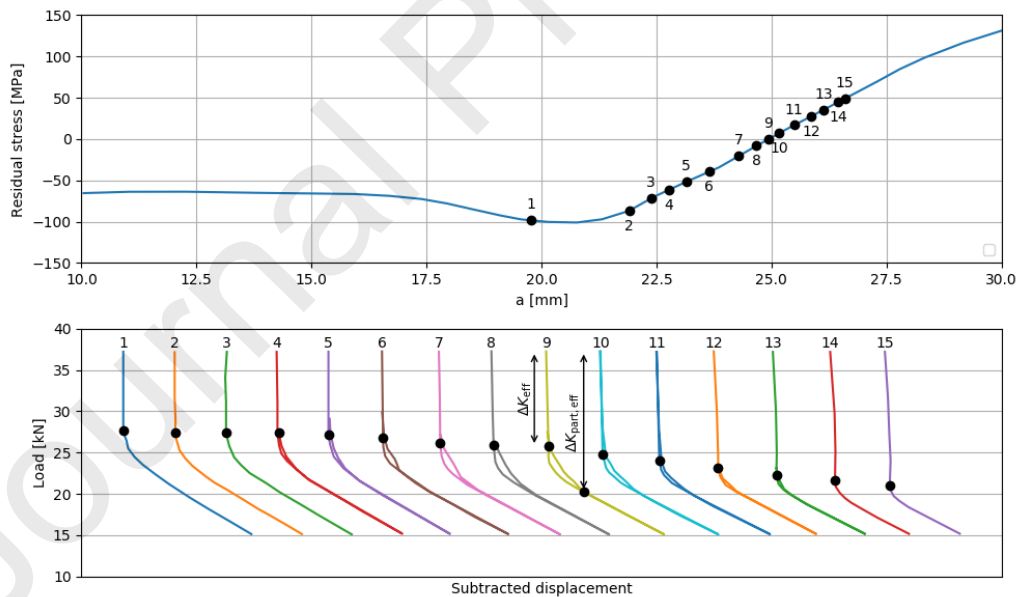


Figure 7: Load versus subtracted displacement curves in the residual stress transition zone. Conventional crack opening load is highlighted as along with the proposed partial opening load for curve 9. Reproduced from [45].

744

745 To summarize, crack closure aims to describe the physical reason for the
746 crack growth stress ratio effects. Residual stresses naturally affect the crack
747 opening stresses, and complex behavior of partial crack opening is reasoned
748 to occur when the crack propagates from a compressive residual stress field
749 to a tensile residual stress field. Similar phenomena were observed after ten-
750 sile overload without macroscopic residual stresses. Generalization of the
751 crack growth assessment to different geometries and in 3D appears to be
752 possible only via numerical analyses (FEM). No studies were found where
753 the crack closure were modeled to take into account the crack tip cyclic con-
754 ditions and combined with strain energy release rate -based criterion (from
755 FEA) to correlate the measurements. The crack growth threshold values
756 in residual stress fields have been paid little attention. Interestingly, the
757 researchers studying crack growth in residual stressed fields have not cited
758 the research conducted on overloads, and they have seemingly independently
759 reached similar conclusions regarding partial crack closure. The proposed
760 analysis methodology is different for these two groups of researchers. The
761 cyclic plastic behavior of the material ahead of crack tip is more pronounced
762 at negative stress ratios in the form of compressive residual stress relaxation.
763 In these situations, the combined effect of residual stresses and crack clo-
764 sure seems to be rather complex, and no simple generalization can be made.
765 Under macroscopic compressive residual stresses, superposition effectively
766 produces negative stress ratios even with positive applied stress ratios. It
767 is not clear, however, whether the effects observed for the negative applied
768 stress ratios apply in the case where applied stress ratio is positive but due to
769 compressive residual stresses the effective stress ratio is negative. Because of
770 the lack of experimental evidence for significant compressive residual stress
771 relaxation due to crack extension, with positive applied load ratio, it would
772 be reasonable to assume that they do not apply.

773 8. Discussion

774 A lot of the practical engineering works with residual stresses utilizes
775 empirically-measured values for fatigue strength improvement or fatigue crack
776 growth rate reduction, more or less directly from the test specimen to the
777 component assessment/validation. Reading the literature quickly reveals
778 that fatigue assessment in the residual stressed state can be complicated.
779 This knowledge is crucial when deciding, for example, whether to try to en-
780 hance the component's fatigue properties by taking advantage of the residual

781 stresses. General guidelines can be given for eliminating the need for more
782 accurate consideration of the residual stresses - like when the service load
783 amplitude clearly causes cyclic plasticity or in a case where the component is
784 exposed to significantly elevated temperatures. In these situations, the role
785 of residual stresses is diminished, and other means for improving the fatigue
786 performance should be considered. Other than those conditions, it is easy to
787 realize that the problem consists of many parts that must be either measured
788 or assumed.

789 The relaxation of the residual stresses could certainly be captured with
790 state-of-the-art constitutive material models. These models have successfully
791 been used to simulate the static relaxation and effects of crack extension on
792 residual stresses. The calculations for cyclic relaxation can get computation-
793 ally expensive, and thus, the role of empirical models in capturing the effects
794 holds. There are, however, a few solver techniques for accelerating the cyclic
795 development in FEA that could be utilized for this purpose. For infinite life
796 approximations, bearing in mind the very high cycle fatigue, the relaxation
797 typically stabilizes, and modeling the static relaxation will suffice.

798 When only finite life is of interest, the problem can be simplified by only
799 considering the macroscopic crack growth phase. Research groups working
800 on fracture mechanics have focused their studies largely on the effects of
801 residual stresses on the fatigue crack growth rate instead of threshold values.
802 The principle of superposition and the weight functions can be used to get
803 rapid estimates. Due to the nature of crack closure, confidence on calcula-
804 tions increases in situations where the measurement scenario is closer to that
805 of the scenario of the real component. The generalization of the methodology
806 always involves measuring the relaxation of residual stresses as well as the
807 crack opening behavior when performing crack growth tests. Furthermore, to
808 get general estimates of the crack closure, sophisticated FEA is required. In
809 these analyses, the cyclic plastic material behavior should be captured with
810 the crack growth scheme and refinement of the mesh. For predictions, crack
811 closure is an essential parameter yielding the physical reason for R -ratio de-
812 pendencies, which are pronounced in the presence of residual stresses and
813 notches. The prediction is based on finding the crack opening stress/load to
814 define the minimum load, and then calculating the effective stress intensity
815 factor range based on that load. In the FEA of partial crack opening, which
816 is suggested to occur after tensile overload and in residual stress gradients,
817 the mouth closing levels were found to better correlate with the measured
818 crack opening levels. It is not clear, however, whether in a simulation ca-

819 pable of capturing the crack closure, it would be more straight-forward to
820 use a strain energy release rate-based criterion. FE analyses seem to answer
821 the need for analyses that can take into account the physical phenomena
822 and derive values closer to the real crack tip driving force, as described by
823 Suresh and Ritchie. Presently, FEA is used only to correlate the measured
824 crack opening stresses, and its full potential in analyzing the crack tip stress
825 history has not been realized yet. The findings at negative stress ratios
826 also emphasize the complex relationship of crack closure, residual stresses,
827 and material's cyclic plastic behavior, which were successfully captured with
828 FEM. Multiaxiality of the residual stresses is typically ignored, and an anal-
829 ysis is performed in the first-mode direction. The role of cold working effects
830 in macroscopic residual stress fields have not been widely considered in crack
831 growth approaches, even though the effects on crack initiation and crack
832 growth rate have been successfully shown with measurements. It would be
833 natural to presume that cold working would alter crack growth curves from
834 non-cold worked, as shown by Jones. The observed non-elliptical cracks in
835 the presence of residual stresses are a clear scenario where the weight function
836 methodology, restricted largely to elliptical cracks, cannot predict accurately.

837 Some fracture mechanics researchers tend to emphasize the importance
838 of keeping the analysis simple. It seems rather difficult to find simple general
839 tools that could serve engineers and researchers alike in fatigue assessment in
840 residual stressed states. Numerical methods (FEM) have been successfully
841 used to analyze these complex phenomena for over 40 years. Increasing the
842 detail in these analyses tend to yield better predictions. The fundamental
843 property that needs to be measured is the material's cyclic plastic proper-
844 ties, which are distinct from those found in the crack growth tests (i.e. can
845 be measured separately and is repeatable). With this, FEM is then capable
846 of delivering estimates for both the residual stresses and plasticity-induced
847 crack closure for cracks of any shape and loading scenario. The pursuit to
848 arrive at one parameter/mechanism (as in crack closure) to explain all the
849 associated phenomena has not been beneficial to the development of analy-
850 sis tools, especially given the difficulties faced in uniquely determining crack
851 closure values and corner cases where compliance based crack opening load
852 does not yield an explanation for the observed phenomena. A typical counter-
853 argument is that *good enough* estimates can be achieved with these simple
854 tools, which is certainly true, especially for engineering works combined with
855 corresponding safety factors. However, for scientific progress in this field and
856 for the advancement of analysis methodology it will be more productive to

857 focus on developing numerical models capable of capturing the distinct phys-
858 ical phenomena observed in these situations. As a more concrete example,
859 the oxide-induced crack closure could be modeled as a time- and loading-
860 dependent evolution equation-based mechanical description of the contact
861 interface. Development of this kind of model then naturally gives rise to
862 questions regarding model parameters and ways to test them. It is our view
863 that the less we have to infer from the experimental crack growth curves, the
864 better. Ideally, the model parameters could be tested separately, like in the
865 case of cyclic plasticity.

866 If a more precise total fatigue life or infinite life prediction is needed, then
867 the crack initiation phase should be analyzed. Unfortunately, we found no
868 studies that base their prediction on systematically measured aspects of the
869 phenomenon: relaxation of residual stresses, changes in surface roughness,
870 effects of cold working, base material fatigue properties, and mean stress
871 sensitivity. Presently, there is no generally accepted fatigue assessment crite-
872 rion. Here, the role of multiaxiality of the residual stresses again seems to be
873 unclear; typically, similar to crack growth, only the residual stresses acting
874 in the direction of the loading were considered, compromising the validity of
875 multiaxial fatigue criteria using hydrostatic stress as a measure for compres-
876 sive mean stress. The hydrostatic mean stress could result in the overestima-
877 tion of the positive effect of compressive residual stresses, paving the way for
878 non-conservative estimates. Hardness measured locally for the cold-worked
879 layers did not prove to be explanatory for the changes in fatigue strength
880 due to cold-working. Extending the methodology to predicting arbitrary
881 components and states again requires the characterization of the material's
882 cyclic plastic behavior and initialization/simulation of the material state due
883 to the residual stress-generating process to capture the Bauschinger's effect
884 properly. Treating residual stresses simply as mean stresses provides a crude
885 estimate for practical engineering purposes. Neglecting the relaxation of
886 residual stresses, effects of cold work, and modifications to surface roughness
887 can lead to non-conservative estimates and as a consequence to an increase
888 in required safety factors in the absence of the quantification of these effects.

889 **9. Acknowledgements**

890 This study was conducted as part of the WIMMA (Dnro 1566/31/2015)
891 -research project. The authors are grateful for the financial support provided
892 by Business Finland Oy (former Tekes) and Wärtsilä Finland Oy. The au-

893 thors are grateful for the fruitful discussions and feedback from Dr. Jouko
894 Hintikka.

895 References

- 896 [1] P. J. Withers, H. Bhadeshia, Residual stress. Part 1–Measurement
897 techniques, *Materials Science and Technology* 17 (4) (2001) 355–365.
898 doi:10.1179/026708301101509980.
- 899 [2] M. James, Residual stress influences on structural reliabil-
900 ity, *Engineering Failure Analysis* 18 (8) (2011) 1909–1920.
901 doi:10.1016/j.engfailanal.2011.06.005.
- 902 [3] R. McClung, A literature survey on the stability and significance of
903 residual stresses during fatigue, *Fatigue & Fracture of Engineering*
904 *Materials & Structures* 30 (3) (2007) 173–205. doi:10.1111/j.1460-
905 2695.2007.01102.x.
- 906 [4] M. Torres, H. Voorwald, An evaluation of shot peening, residual stress
907 and stress relaxation on the fatigue life of AISI 4340 steel, *Internation-*
908 *al Journal of Fatigue* 24 (8) (2002) 877–886. doi:10.1016/S0142-
909 1123(01)00205-5.
- 910 [5] K. Shiozawa, L. Lu, Very high-cycle fatigue behaviour of shot-peened
911 high-carbon–chromium bearing steel, *Fatigue & Fracture of Engineer-*
912 *ing Materials & Structures* 25 (8-9) (2002) 813–822. doi:10.1046/j.1460-
913 2695.2002.00567.x.
- 914 [6] T. Klotz, D. Delbergue, P. Bocher, M. Lévesque, M. Brochu,
915 Surface characteristics and fatigue behavior of shot peened In-
916 conel 718, *International Journal of Fatigue* 110 (2018) 10–21.
917 doi:10.1016/j.ijfatigue.2018.01.005.
- 918 [7] W. Z. Zhuang, G. R. Halford, Investigation of residual stress relaxation
919 under cyclic load, *International Journal of Fatigue* 23 (2001) 31–37.
920 doi:10.1016/S0142-1123(01)00132-3.
- 921 [8] S. Bagherifard, R. Ghelichi, M. Guagliano, On the shot peening surface
922 coverage and its assessment by means of finite element simulation: a
923 critical review and some original developments, *Applied Surface Science*
924 259 (2012) 186–194. doi:10.1016/j.apsusc.2012.07.017.

- 925 [9] A. C. Rufin, Extending the fatigue life of aircraft engine components
926 by hole cold expansion technology, *Journal of Engineering for Gas Tur-*
927 *bines and Power* 115 (1) (1993) 165–171. doi:10.1115/1.2906672.
- 928 [10] A. Özdemir, L. Edwards, Relaxation of residual stresses at cold-
929 worked fastener holes due to fatigue loading, *Fatigue & Fracture*
930 *of Engineering Materials & Structures* 20 (10) (1997) 1443–1451.
931 doi:10.1243/03093247V316413.
- 932 [11] J. Mann, A. Machin, W. Lupson, R. Pell, The use of interference-fit
933 bolts or bushes and hole cold expansion for increasing the fatigue life
934 of thick-section aluminium alloy bolted joints, Tech. rep., AERONAU-
935 TICAL RESEARCH LABS MELBOURNE (AUSTRALIA) (1983).
936 URL <http://www.dtic.mil/docs/citations/ADA142083>
- 937 [12] D. Stefanescu, M. Dutta, D. Wang, L. Edwards, M. Fitzpatrick, The
938 effect of high compressive loading on residual stresses and fatigue crack
939 growth at cold expanded holes, *The Journal of Strain Analysis for Engi-*
940 *neering Design* 38 (5) (2003) 419–427. doi:10.1243/03093240360713478.
- 941 [13] M. Kattoura, S. R. Mannava, D. Qian, V. K. Vasudevan, Effect of laser
942 shock peening on residual stress, microstructure and fatigue behavior
943 of ATI 718Plus alloy, *International Journal of Fatigue* 102 (2017) 121–
944 134. doi:10.1016/j.ijfatigue.2017.04.016.
- 945 [14] S. Keller, M. Horstmann, N. Kashaev, B. Klusemann, Experimen-
946 tally validated multi-step simulation strategy to predict the fa-
947 tigue crack propagation rate in residual stress fields after laser
948 shock peening, *International Journal of Fatigue* 124 (2019) 265–276.
949 doi:10.1016/j.ijfatigue.2018.12.014.
- 950 [15] P. Prevéy, J. Telesman, T. Gabb, P. Kantzos, FOD resistance and
951 fatigue crack arrest in low plasticity burnished IN718, in: *Proceedings*
952 *of the 5th Nat. Turbine Eng. HCF Conference*, 2000.
953 URL <https://www.lambdatechs.com/wp-content/uploads/221.pdf>
- 954 [16] A. H. Clauer, Laser shock peening for fatigue resistance, *Surface per-*
955 *formance of titanium* 217 (1996) 230.
- 956 [17] Y. Guo, W. Li, I. Jawahir, Surface integrity characterization and pre-
957 diction in machining of hardened and difficult-to-machine alloys: a

- 958 state-of-art research review and analysis, *Machining Science and Tech-*
959 *nology* 13 (4) (2009) 437–470. doi:10.1080/10910340903454922.
- 960 [18] R. M'Saoubi, J. Outeiro, H. Chandrasekaran, O. Dillon Jr, I. Jawahir,
961 A review of surface integrity in machining and its impact on
962 functional performance and life of machined products, *International*
963 *Journal of Sustainable Manufacturing* 1 (1-2) (2008) 203–236.
964 doi:10.1504/IJSM.2008.019234.
- 965 [19] S. Saini, I. S. Ahuja, V. S. Sharma, Residual stresses, surface
966 roughness, and tool wear in hard turning: a comprehensive re-
967 view, *Materials and Manufacturing Processes* 27 (6) (2012) 583–598.
968 doi:10.1080/10426914.2011.585505.
- 969 [20] W. Ding, L. Zhang, Z. Li, Y. Zhu, H. Su, J. Xu, Review on grinding-
970 induced residual stresses in metallic materials, *The International Jour-*
971 *nal of Advanced Manufacturing Technology* 88 (9-12) (2017) 2939–
972 2968. doi:10.1007/s00170-016-8998-1.
- 973 [21] J. Rohde, A. Jeppsson, Literature review of heat treatment simu-
974 lations with respect to phase transformation, residual stresses and
975 distortion, *Scandinavian Journal of Metallurgy* 29 (2) (2000) 47–62.
976 doi:10.1034/j.1600-0692.2000.d01-6.x.
- 977 [22] Y. Rong, J. Xu, Y. Huang, G. Zhang, Review on finite ele-
978 ment analysis of welding deformation and residual stress, *Science*
979 *and Technology of Welding and Joining* 23 (3) (2018) 198–208.
980 doi:10.1080/13621718.2017.1361673.
- 981 [23] P. Dong, F. Brust, Welding residual stresses and effects on frac-
982 ture in pressure vessel and piping components: a millennium re-
983 view and beyond, *J. Pressure Vessel Technol.* 122 (3) (2000) 329–338.
984 doi:10.1115/1.556189.
- 985 [24] C. Sonsino, Effect of residual stresses on the fatigue behaviour
986 of welded joints depending on loading conditions and weld ge-
987 ometry, *International Journal of Fatigue* 31 (1) (2009) 88–101.
988 doi:10.1016/j.ijfatigue.2008.02.015.
- 989 [25] T.-L. Teng, C.-P. Fung, P.-H. Chang, Effect of weld geometry and resid-
990 ual stresses on fatigue in butt-welded joints, *International Journal of*

- 991 Pressure Vessels and Piping 79 (7) (2002) 467–482. doi:10.1016/S0308-
992 0161(02)00060-1.
- 993 [26] C.-H. Lee, K.-H. Chang, Temperature fields and residual stress
994 distributions in dissimilar steel butt welds between carbon and
995 stainless steels, Applied Thermal Engineering 45 (2012) 33–41.
996 doi:10.1016/j.applthermaleng.2012.04.007.
- 997 [27] V. N. Van Do, C.-H. Lee, K.-H. Chang, High cycle fatigue anal-
998 ysis in presence of residual stresses by using a continuum damage
999 mechanics model, International Journal of Fatigue 70 (2015) 51–62.
1000 doi:10.1016/j.ijfatigue.2014.08.013.
- 1001 [28] F. Shen, B. Zhao, L. Li, C. K. Chua, K. Zhou, Fatigue damage evo-
1002 lution and lifetime prediction of welded joints with the consideration
1003 of residual stresses and porosity, International Journal of Fatigue 103
1004 (2017) 272–279. doi:10.1016/j.ijfatigue.2017.06.014.
- 1005 [29] J.-C. Kim, S.-K. Cheong, H. Noguchi, Residual stress relaxation
1006 and low-and high-cycle fatigue behavior of shot-peened medium-
1007 carbon steel, International Journal of Fatigue 56 (2013) 114–122.
1008 doi:10.1016/j.ijfatigue.2013.07.001.
- 1009 [30] J.-C. Kim, S.-K. Cheong, H. Noguchi, Proposed fatigue damage mea-
1010 surement parameter for shot-peened carbon steel based on fatigue crack
1011 growth behavior, International Journal of Fatigue 74 (2015) 97–106.
1012 doi:10.1016/j.ijfatigue.2014.12.016.
- 1013 [31] H.-C. Choi, J.-H. Song, Finite element analysis of closure behaviour of
1014 fatigue cracks in residual stress fields, Fatigue & Fracture of Engineer-
1015 ing Materials & Structures 18 (1) (1995) 105–117. doi:10.1111/j.1460-
1016 2695.1995.tb00145.x.
- 1017 [32] M. Pavier, C. Poussard, D. Smith, Finite element modelling
1018 of the interaction of residual stress with mechanical load for a
1019 crack emanating from a cold worked fastener hole, The Journal
1020 of Strain Analysis for Engineering Design 33 (4) (1998) 275–289.
1021 doi:10.1243/0309324981512995.

- 1022 [33] G. Webster, A. Ezeilo, Residual stress distributions and their influence
1023 on fatigue lifetimes, *International Journal of Fatigue* 23 (2001) 375–383.
1024 doi:10.1016/S0142-1123(01)00133-5.
- 1025 [34] J. Toribio, M. Lorenzo, D. Vergara, L. Aguado, Residual stress re-
1026 distribution induced by fatigue in cold-drawn prestressing steel wires,
1027 *Construction and Building Materials* 114 (2016) 317–322.
- 1028 [35] J. Toribio, M. Lorenzo, D. Vergara, L. Aguado, The role of overload-
1029 ing on the reduction of residual stress by cyclic loading in cold-drawn
1030 prestressing steel wires, *Applied Sciences* 7 (1) (2017) 84.
- 1031 [36] S. Kodama, The behavior of residual stress during fatigue stress cycles,
1032 in: *Proceedings of the International Conference on Mechanical Behav-*
1033 *ior of Metals II*, Society of Material Science, Kyoto, Vol. 2, 1972, pp.
1034 111–118.
- 1035 [37] D. Kirk, Effects of plastic straining on residual stresses induced by
1036 shot-peening.(Retroactive coverage), *Shot Peening: Science, Technol-*
1037 *ogy* (1987) 213–220.
1038 URL <https://www.shotpeener.com/library/detail.php?anc=1987025>
- 1039 [38] L. Wagner, G. Luetjering, Influence of shot peening on the fatigue
1040 behavior of titanium alloys, in: *Proceedings of the First International*
1041 *Conference on Shot Peening*, Paris, France, 1996, pp. 453–460.
1042 URL <https://www.shotpeener.com/library/pdf/1981036.pdf>
- 1043 [39] O. Vöhringer, T. Hirsch, E. Macherauch, Relaxation of shot peening
1044 induced residual stresses of TiAl 6 V 4 by annealing or mechanical
1045 treatment, *Titanium: Science and technology* (1985) 2203–2210.
- 1046 [40] S. Fukuda, Y. Tsuruta, An experimental study of redistribution of
1047 welding residual stress with fatigue crack extension, *Transactions of*
1048 *JWRI* 7 (2) (1978) 215–220.
1049 URL <http://hdl.handle.net/11094/10170>
- 1050 [41] Y.-B. Lee, C.-S. Chung, Y.-K. Park, H.-K. Kim, Effects of redistribut-
1051 ing residual stress on the fatigue behavior of SS330 weldment, *Inter-*
1052 *national Journal of Fatigue* 20 (8) (1998) 565–573. doi:10.1016/S0142-
1053 1123(98)00024-3.

- 1054 [42] Y. Lam, K. Lian, The effect of residual stress and its redistribution
1055 of fatigue crack growth, *Theoretical and Applied Fracture Mechanics*
1056 12 (1) (1989) 59–66. doi:10.1016/0167-8442(89)90015-3.
- 1057 [43] M. Pavier, C. Poussard, D. Smith, Effect of residual stress around cold
1058 worked holes on fracture under superimposed mechanical load, *Engi-
1059 neering Fracture Mechanics* 63 (6) (1999) 751–773. doi:10.1016/S0013-
1060 7944(99)00050-8.
- 1061 [44] D. Nelson, Effects of residual stress on fatigue crack propagation,
1062 in: *Residual stress effects in fatigue*, ASTM International, 1982.
1063 doi:10.1520/STP30104S.
- 1064 [45] K. J. Kang, J. H. Song, Y. Y. Earmme, Fatigue crack growth and
1065 closure behaviour through a compressive residual stress field, *Fatigue
1066 & Fracture of Engineering Materials & Structures* 13 (1) (1990) 1–13.
1067 doi:10.1111/j.1460-2695.1990.tb00572.x.
- 1068 [46] K. Amjad, D. Asquith, E. A. Patterson, C. M. Sebastian, W.-C.
1069 Wang, The interaction of fatigue cracks with a residual stress field
1070 using thermoelastic stress analysis and synchrotron X-ray diffrac-
1071 tion experiments, *Royal Society Open Science* 4 (11) (2017) 171100.
1072 doi:10.1098/rsos.171100.
- 1073 [47] V. Kliman, M. Bily, J. Prohacka, Improvement of fatigue performance
1074 by cold hole expansion. Part 1: Model of fatigue limit improvement, *In-
1075 ternational Journal of Fatigue* 15 (2) (1993) 93–100. doi:10.1016/0142-
1076 1123(93)90003-9.
- 1077 [48] E. Wolf, Fatigue crack closure under cyclic tension, *Engineering Frac-
1078 ture Mechanics* 2 (1) (1970) 37–45. doi:10.1016/0013-7944(70)90028-7.
- 1079 [49] R. Pippin, A. Hohenwarter, Fatigue crack closure: a review of the
1080 physical phenomena, *Fatigue & Fracture of Engineering Materials &
1081 Structures* 40 (4) (2017) 471–495. doi:10.1111/ffe.12578.
- 1082 [50] S. Suresh, *Near-threshold fatigue crack propagation: a perspective on
1083 the role of crack closure*, The Metallurgical Society of AIME, Warren-
1084 dale, PA, 1984.
1085 URL <https://escholarship.org/uc/item/8mr83283>

- 1086 [51] N. Fleck, R. Smith, Crack closure- is it just a surface phenomenon., In-
1087 ternational Journal of Fatigue 4 (3) (1982) 157–160. doi:10.1016/0142-
1088 1123(82)90043-3.
- 1089 [52] J. Newman, A crack-closure model for predicting fatigue crack growth
1090 under aircraft spectrum loading, in: Methods and models for predicting
1091 fatigue crack growth under random loading, ASTM International, 1981.
1092 doi:10.1520/STP28334S.
- 1093 [53] R. McClung, B. Thacker, S. Roy, Finite element visualization of fatigue
1094 crack closure in plane stress and plane strain, International Journal of
1095 Fracture 50 (1) (1991) 27–49. doi:10.1007/BF00035167.
- 1096 [54] E. Salvati, H. Zhang, K. S. Fong, X. Song, A. M. Korsunsky, Separating
1097 plasticity-induced closure and residual stress contributions to fatigue
1098 crack retardation following an overload, Journal of the Mechanics and
1099 Physics of Solids 98 (2017) 222–235. doi:10.1016/j.jmps.2016.10.001.
- 1100 [55] R. McClung, Finite element analysis of specimen geometry effects
1101 on fatigue crack closure, Fatigue & Fracture of Engineering Ma-
1102 terials & Structures 17 (8) (1994) 861–872. doi:10.1111/j.1460-
1103 2695.1994.tb00816.x.
- 1104 [56] R. McClung, H. Sehitoglu, On the finite element analysis of fatigue
1105 crack closure. II. Numerical results, Eng. Fract. Mech. 33 (2) (1989)
1106 253–272. doi:10.1016/0013-7944(89)90028-3.
- 1107 [57] S. Pommier, P. Bompard, Bauschinger effect of alloys and plasticity-
1108 induced crack closure: a finite element analysis, Fatigue Fracture
1109 of Engineering Materials and Structures 23 (2) (2000) 129–139.
1110 doi:10.1046/j.1460-2695.2000.00259.x.
- 1111 [58] D. Camas, J. Garcia-Manrique, B. Moreno, A. Gonzalez-Herrera, Nu-
1112 merical modelling of three-dimensional fatigue crack closure: Mesh
1113 refinement, International Journal of Fatigue 113 (2018) 193–203.
1114 doi:10.1016/j.ijfatigue.2018.03.035.
- 1115 [59] S. Pommier, C. Prioul, P. Bompard, Influence of a negative R ratio on
1116 the creep-fatigue behaviour of the N18 nickel base superalloy, Fatigue
1117 & Fracture of Engineering Materials & Structures 20 (1) (1997) 93–107.
1118 doi:10.1111/j.1460-2695.1997.tb00405.x.

- 1119 [60] F. Silva, Crack closure inadequacy at negative stress ratios, *International Journal of Fatigue* 26 (3) (2004) 241–252. doi:10.1016/S0142-
1120 1123(03)00162-2.
1121
- 1122 [61] J. Rice, Mechanics of crack tip deformation and extension by fa-
1123 tigue, in: *Fatigue crack propagation*, ASTM International, 1967.
1124 doi:10.1520/STP47234S.
- 1125 [62] M. Thielen, F. Schaefer, P. Gruenewald, M. Laub, M. Marx,
1126 M. Meixner, M. Klaus, C. Motz, In situ synchrotron stress
1127 mappings to characterize overload effects in fatigue crack
1128 growth, *International Journal of Fatigue* 121 (2019) 155–162.
1129 doi:10.1016/j.ijfatigue.2018.12.013.
- 1130 [63] R. E. Jones, Fatigue crack growth retardation after single-cycle peak
1131 overload in Ti-6Al-4V titanium alloy, *Engineering Fracture Mechanics*
1132 5 (3) (1973) 585–604. doi:10.1016/0013-7944(73)90042-8.
- 1133 [64] C. Robin, M. e. Louah, G. Pluinage, Influence of an overload on
1134 the fatigue crack growth in steels, *Fatigue & Fracture of Engineer-
1135 ing Materials & Structures* 6 (1) (1983) 1–13. doi:10.1111/j.1460-
1136 2695.1983.tb01135.x.
- 1137 [65] H. Shercliff, N. Fleck, Effect of specimen geometry on fatigue crack
1138 growth in plane strain - II. Overload response, *Fatigue & Frac-
1139 ture of Engineering Materials & Structures* 13 (3) (1990) 297–310.
1140 doi:10.1111/j.1460-2695.1990.tb00601.x.
- 1141 [66] P. C. Paris, H. Tada, J. K. Donald, Service load fatigue damage - a
1142 historical perspective, *International Journal of Fatigue* 21 (1999) S35–
1143 S46. doi:10.1016/S0142-1123(99)00054-7.
- 1144 [67] L. Borrego, J. Ferreira, J. P. Da Cruz, J. Costa, Evaluation of overload
1145 effects on fatigue crack growth and closure, *Engineering Fracture Me-
1146 chanics* 70 (11) (2003) 1379–1397. doi:10.1016/S0013-7944(02)00119-4.
- 1147 [68] M. Halliday, J. Zhang, P. Poole, P. Bowen, In situ SEM observations
1148 of the contrasting effects of an overload on small fatigue crack growth
1149 at two different load ratios in 2024-T351 aluminium alloy, *Internation-
1150 al Journal of Fatigue* 19 (4) (1997) 273–282. doi:10.1016/S0142-
1151 1123(97)00010-8.

- 1152 [69] C. Makabe, A. Purnowidodo, A. McEvily, Effects of surface deforma-
1153 tion and crack closure on fatigue crack propagation after overloading
1154 and underloading, *International Journal of Fatigue* 26 (12) (2004) 1341–
1155 1348. doi:10.1016/j.ijfatigue.2004.03.017.
- 1156 [70] F. Silva, Fatigue crack propagation after overloading and underloading
1157 at negative stress ratios, *International Journal of Fatigue* 29 (9-11)
1158 (2007) 1757–1771. doi:10.1016/j.ijfatigue.2007.03.012.
- 1159 [71] K. Sadananda, A. Vasudevan, Short crack growth and internal
1160 stresses, *International Journal of Fatigue* 19 (93) (1997) 99–108.
1161 doi:10.1016/S0142-1123(97)00057-1.
- 1162 [72] A. Vasudeven, K. Sadananda, N. Louat, A review of crack clo-
1163 sure, fatigue crack threshold and related phenomena, *Materials Sci-
1164 ence and Engineering: A* 188 (1-2) (1994) 1–22. doi:10.1016/0921-
1165 5093(94)90351-4.
- 1166 [73] R. Pell, P. Beaver, J. Mann, J. Sparrow, Fatigue of thick-section
1167 cold-expanded holes with and without cracks, *Fatigue & Frac-
1168 ture of Engineering Materials & Structures* 12 (6) (1989) 553–567.
1169 doi:10.1111/j.1460-2695.1989.tb00563.x.
- 1170 [74] M. T. Kokaly, J. S. Ransom, J. H. Restis, L. Reid, Observations and
1171 analysis of fatigue crack growth from cold expanded holes, in: *Proceed-
1172 ings of the 8th Joint NASA/FAA/DoD Conference on Aging Aircraft,*
1173 2005.
1174 URL <http://www.fatiguetechnology.com/PDF/EL013.pdf>
- 1175 [75] J. Liu, C. Xiang, H. Yuan, Prediction of 3D small fatigue crack prop-
1176 agation in shot-peened specimens, *Computational Materials Science*
1177 46 (3) (2009) 566–571. doi:10.1016/j.commatsci.2009.03.011.
- 1178 [76] M. Leitner, R. Aigner, D. Dobberke, Local fatigue strength assess-
1179 ment of induction hardened components based on numerical manufact-
1180 uring process simulation, *Procedia Engineering* 213 (2018) 644–650.
1181 doi:10.1016/j.proeng.2018.02.060.
- 1182 [77] R. Smith, P. Watson, T. Topper, A stress-strain function for the fatigue
1183 of metals, *Journal of Materials* 5 (1970) 767–778.

- 1184 [78] C. Boller, T. Seeger, *Materials data for cyclic loading: low-alloy steels*,
1185 Vol. 42, Elsevier, 2013.
- 1186 [79] V. Kliman, M. Bílý, J. Prohacka, Improvement of fatigue performance
1187 by cold hole expansion. Part 2: Experimental verification of pro-
1188 posed model, *International Journal of Fatigue* 15 (2) (1993) 101–107.
1189 doi:10.1016/0142-1123(93)90004-A.
- 1190 [80] R. Fathallah, A. Laamouri, H. Sidhom, C. Braham, High cycle fatigue
1191 behavior prediction of shot-peened parts, *International Journal of Fa-
1192 tigue* 26 (10) (2004) 1053–1067. doi:10.1016/j.ijfatigue.2004.03.007.
- 1193 [81] K. Dang-Van, Macro-micro approach in high-cycle multiaxial fa-
1194 tigue, in: *Advances in multiaxial fatigue*, ASTM International, 1993.
1195 doi:10.1520/STP24799S.
- 1196 [82] J. Lemaitre, *A course on damage mechanics*, Springer Science & Busi-
1197 ness Media, 2012. doi:10.1007/978-3-642-18255-6.
- 1198 [83] R. G. Budynas, J. K. Nisbett, et al., *Shigley’s mechanical engineering
1199 design*, 8th Edition, Vol. 8, McGraw-Hill New York, 2008.
- 1200 [84] I. F. Pariente, M. Guagliano, About the role of residual stresses and
1201 surface work hardening on fatigue ΔK_{th} of a nitrided and shot peened
1202 low-alloy steel, *Surface and Coatings Technology* 202 (13) (2008) 3072–
1203 3080. doi:10.1016/j.surfcoat.2007.11.015.
- 1204 [85] Y. Murakami, *Metal fatigue: effects of small defects and nonmetallic
1205 inclusions*, Elsevier, 2002. doi:10.1016/B978-0-08-044064-4.X5000-2.
- 1206 [86] A. Avilés, R. Avilés, J. Albizuri, L. Pallarés-Santasmartas,
1207 A. Rodríguez, Effect of shot-peening and low-plasticity burnish-
1208 ing on the high-cycle fatigue strength of DIN 34CrNiMo6 al-
1209 loy steel, *International Journal of Fatigue* 119 (2019) 338–354.
1210 doi:10.1016/j.ijfatigue.2018.10.014.
- 1211 [87] S. Bagherifard, C. Colombo, M. Guagliano, Application of different fa-
1212 tigue strength criteria to shot peened notched components. Part 1:
1213 Fracture mechanics based approaches, *Applied Surface Science* 289
1214 (2014) 180–187. doi:10.1016/j.apsusc.2013.10.131.

- 1215 [88] D. Taylor, The theory of critical distances, Engi-
1216 neering Fracture Mechanics 75 (7) (2008) 1696–1705.
1217 doi:10.1016/j.engfracmech.2007.04.007.
- 1218 [89] G. Sines, Failure of materials under combined repeated stresses with
1219 superimposed static stresses.
1220 URL <https://ntrs.nasa.gov/search.jsp?R=19930087814>
- 1221 [90] A. Buch, Fatigue strength calculation, no. 6, Trans Tech Pubn, 1988.
1222 doi:10.1002/crat.2170231016.
- 1223 [91] B. Atzori, P. Lazzarin, G. Meneghetti, A unified treatment of the mode
1224 I fatigue limit of components containing notches or defects, Interna-
1225 tional Journal of Fracture 133 (1) (2005) 61–87. doi:10.1007/s10704-
1226 005-2183-0.
- 1227 [92] S. Bagherifard, M. Guagliano, Application of different fatigue strength
1228 criteria on shot peened notched parts. Part 2: nominal and lo-
1229 cal stress approaches, Applied Surface Science 289 (2014) 173–179.
1230 doi:10.1016/j.apsusc.2013.10.130.
- 1231 [93] W. Eichseder, Fatigue analysis by local stress concept based on finite
1232 element results, Computers & Structures 80 (27-30) (2002) 2109–2113.
1233 doi:10.1016/S0045-7949(02)00273-0.
- 1234 [94] F. Maschinenbau, E. Haibach, Analytical strength assessment of com-
1235 ponents in mechanical engineering, VDMA-Verlag, 2003.
- 1236 [95] B. Gerin, E. Pessard, F. Morel, C. Verdu, A non-local approach to
1237 model the combined effects of forging defects and shot-peening on the
1238 fatigue strength of a pearlitic steel, Theoretical and Applied Fracture
1239 Mechanics 93 (2018) 19–32. doi:10.1016/j.tafmec.2017.06.012.
- 1240 [96] B. Gerin, E. Pessard, F. Morel, C. Verdu, Influence of surface integrity
1241 on the fatigue behaviour of a hot-forged and shot-peened C70 steel
1242 component, Materials Science and Engineering: A 686 (2017) 121–133.
1243 doi:10.1016/j.msea.2017.01.041.
- 1244 [97] H. Bueckner, Novel principle for the computation of stress intensity
1245 factors, Zeitschrift fuer Angewandte Mathematik & Mechanik 50 (9).

- 1246 [98] A. Parker, Stress intensity factors, crack profiles, and fatigue crack
1247 growth rates in residual stress fields, in: Residual stress effects in fa-
1248 tigue, ASTM International, 1982. doi:10.1520/STP30095S.
- 1249 [99] A. Todoroki, H. Kobayashi, Prediction of fatigue crack
1250 growth rate in residual stress fields, in: Key Engineering
1251 Materials, Vol. 51, Trans Tech Publ, 1991, pp. 367–372.
1252 doi:10.4028/www.scientific.net/KEM.51-52.367.
- 1253 [100] M. Beghini, L. Bertini, Fatigue crack propagation through residual
1254 stress fields with closure phenomena, Engineering Fracture Mechanics
1255 36 (3) (1990) 379–387. doi:10.1016/0013-7944(90)90285-O.
- 1256 [101] M. Pavan, D. Furfari, B. Ahmad, M. Gharghouri, M. Fitz-
1257 patrick, Fatigue crack growth in a laser shock peened residual
1258 stress field, International Journal of Fatigue 123 (2019) 157–167.
1259 doi:10.1016/j.ijfatigue.2019.01.020.
- 1260 [102] M. Beghini, L. Bertini, E. Vitale, Fatigue crack growth in residual
1261 stress fields: experimental results and modelling, Fatigue & Frac-
1262 ture of Engineering Materials & Structures 17 (12) (1994) 1433–1444.
1263 doi:10.1111/j.1460-2695.1994.tb00786.x.
- 1264 [103] A. Parker, D. Nelson, Discussion, in: Residual stress effects in fatigue,
1265 ASTM International, 1982.
- 1266 [104] O. E. Wheeler, Spectrum loading and crack growth, Journal of Basic
1267 Engineering 94 (1) (1972) 181–186. doi:10.1115/1.3425362.
- 1268 [105] J. Willenborg, R. Engle, H. Wood, A crack growth retardation model
1269 using an effective stress concept, Tech. rep., Air Force Flight Dynamics
1270 Lab Wright-Patterson Afb Oh (1971).
1271 URL <http://www.dtic.mil/docs/citations/ADA956517>
- 1272 [106] W. Elber, The significance of fatigue crack closure, ASTM International
1273 (1971) 230–242. doi:10.1520/STP26680S.
- 1274 [107] J. Newman, A crack opening stress equation for fatigue crack
1275 growth, International Journal of Fracture 24 (4) (1984) R131–R135.
1276 doi:10.1007/BF00020751.

- 1277 [108] R. G. Forman, S. R. Mettu, Behavior of surface and corner cracks
1278 subjected to tensile and bending loads in Ti-6Al-4V alloy.
1279 URL <https://ntrs.nasa.gov/search.jsp?R=19910009960>
- 1280 [109] Y. Mukai, A proposal for stress intensity factor range calculation
1281 method by partial opening model of fatigue crack under weld residual
1282 stress field and prediction of the crack propagation behaviour, Journal
1283 of JWS 5 (2) (1987) 85–88.

- Hydrostatic compressive residual stress might result in non-conservative estimates
- Cold-working effects on fatigue strength are typically neglected
- Numerical methods have improved estimates of crack closure and residual stresses

Journal Pre-proofs